(1)

ULTRA-FAST TUNABLE MICROWAVE FILTER
PHASE II, TASK 1

Adolph Presser
RCA Laboratories
David Sarnoff Research Center
Princeton, New Jersey 08540

28 AUGUST 1980

Final Report for Period I June, 1979 to 15 May, 1980

Prepared for
Department of the Navy
Naval Research Laboratory
Washington, D.C. 20375

REPORT DOCUMENTATION PAGE

READ INSTRUCTIONS BEFORE COMPLETING FORM

1. REPORT NUMBER	2. GOVT ACCESSION NO. / 3. RECIPIENT'S CATALOG NUMBER
4. TITLE (and Subtitle): ULTRAFAST TUNABLE MICROWAVE FILTER	5. TYPE OF REPORT & PERIOD COVERED: Final Report (6-1-79 to 5-15-80)
	6. PERFORMING ORG. REPORT NUMBER: PRRL-80-CR-41
7. AUTHOR(s): A. Presser	8. CONTRACT OR GRANT NUMBER(s): N00173-79-C-0186
9. PERFORMING ORGANIZATION NAME AND ADDRESS: RCA Laboratories, Princeton, New Jersey 08540	10. PROGRAM ELEMENT, PROJECT, TASK AREA & WORK UNIT NUMBERS
11. CONTROLLING OFFICE NAME AND ADDRESS: Department of the Navy, Naval Research Laboratory, Washington, DC 20375	12. REPORT DATE: August 1980
	13. NUMBER OF PAGES: 48
14. MONITORING AGENCY NAME & ADDRESS (if different from Controlling Office)	15. SECURITY CLASS. (of this report): Unclassified
	15a. DECLASSIFICATION/DOWNGRADING SCHEDULE: N/A

16. DISTRIBUTION STATEMENT (of this Report)

APPROVED FOR PUBLIC RELEASE
DISTRIBUTION UNLIMITED

17. DISTRIBUTION STATEMENT (of the abstract entered in Block 20, if different from Report)

18. SUPPLEMENTARY NOTES

19. KEY WORDS (Continue on reverse side if necessary and identify by block number)

Filter
Voltage tunable
Varactor
FET three-section filter

20. ABSTRACT (Continue on reverse side if necessary and identify by block number)

Varactor-tunable resonant filter elements that use the negative resistance of an FET to overcome the losses of the varactor and the circuitry were used to construct two three-section filters.

One filter operates in the tunable frequency range from 8.4 to 9.2 GHz; a second filter, in the required 9.1- to 9.6-GHz frequency range. Midband insertion loss is typically 0 dB; 3-dB bandwidth is 100 MHz.

PREFACE

This interim report describes the work done at the Microwave Technology Center of RCA Laboratories during the period June 1, 1979 to May 15, 1980 in performance of a Phase II, Task 1 program, sponsored by the Naval Electronics System Command, directed by the Naval Research Laboratory under Contract Number N00173-79-C-0186. F. Sterzer is the Center's Director, E. F. Belohoubek was the Project Supervisor, and A. Presser was the Project Scientist.

A-1

TABLE OF CONTENTS

LIST OF ILLUSTRATIONS

LIST OF ILLUSTRATIONS (Continued)

LIST OF ILLUSTRATIONS (Continued)

LIST OF TABLES

SECTION I

INTRODUCTION

During an earlier Phase I program (Contract N00173-77-C-0201), it was demonstrated that the losses in a varactor tuned filter at X-band frequencies can be overcome by the negative resistance of a GaAs FET. This achievement makes an electronically tunable filter with rapid tuning characteristics for ESM systems feasible.

The goals of this Phase II, Task 1 program were to use the approaches of Phase I in the design of a three-section tunable filter with the following performance:

	Goal	Attained
Frequency	9.1-9.6 GHz	9.0-9.6 GHz
Filter Pass Band (BW)	30 MHz	80-120 MHz
Pass Band Insertion Loss	<3 dB	0 dB
Power Input	$\leq$ -10 dBm	-20 dBm
Rejection ($F_o \pm 2$ BW)	-30 dB	-30 dB
Tuning Voltage	0-30 V	0-30 V
RF Connectors	SMA	--
Size	40x40x20 mm	55x52x17 mm
Weight	50 g	175 g

Two three-section filters were constructed and tested. The first of these filters was left to operate at the originally obtained 8.4 GHz to 9.2 GHz tuning range. The second unit was tuned to meet the desired 9.1 GHz to 9.6 GHz frequency range. Typically attained performance is listed above, together with the goal specifications.

The results deviate from the goals mainly in 3 dB bandwidth, size, and weight. The 3 dB bandwidth deviation is caused by the present lack of control over coupling and loading parameters. The size represents an over-sized enclosure selected for construction convenience; removing unnecessary lines within the structure a 40 x 32 x 17 mm enclosure is sufficient. The weight of 175 g is the one for a solid brass structure, scaling to alumina the weight of the oversized structure is 58 grams.

Upon NRL's request, a two-section filter was constructed in addition to the required three-section filters. This additional filter was delivered in March, 1980, ahead of required hardware delivery and was intended for tuning experiments by NRL in anticipation of a particular systems application.

SECTION II

FILTER DESIGN

The basic building block in multi-section filter design in the chosen approach is a tunable resonant filter element. A number, N, of such elements when combined with suitable coupling networks constitutes an N-section filter. In order to be fast tunable, the elements make use of a varactor. The relatively high losses of the varactor, which present a selectivity limitation at microwave frequencies, are overcome by the addition of a GaAs FET that provides a negative resistance. The major design considerations for such an element were described in detail in the final report of Phase I.[1] The following paragraphs describe supporting design work leading to the construction of the resonant element and of multisection filters.

1. FET Model

The attainment of negative resistance with an FET requires interconnection of the device in a specific feedback arrangement on a specific carrier. The mathematical circuit description of an FET model, suitable to be used in computer circuit analysis programs, greatly speeds not only design in the frequency range of interest but also allows one to predict ranges of instability and to check reasons for observed instabilities. One method found to be adequate for FET modeling is to measure the S-parameters of the FET on a carrier with known mounting parasitics.[2] The carrier and mounting parasitics are via computer eliminated from the measured values and after a conversion (S to Y), the values of the FET equivalent circuit parameters, as shown in Figure 1, can be derived. In the simple model, device parameters are assumed not to be frequency dependent, so that evaluation at lower frequencies is sufficient.

The effectiveness of this method is depicted in Figures 2 through 9, which show the measured and calculated magnitudes and phases of all four S-parameters over the 2-10 GHz frequency range. Even though the equivalent parameters were derived from measured values in the .1 to 2 GHz frequency range, the agreement with values at higher frequencies is good. The model was extensively used in the design of the resonant element.

2. Element Construction

The resonant element developed during the Phase I effort is not easily usable in a multisection filter design.[1] The planar redesign was realized

in the form that is shown in Figure 10. Mounting pads for support of the varactor, FET, and various capacitors were etched on a 3.8 x 3.2 x .635 mm alumina wafer. The approximate equivalent circuit is also shown in Figure 10. This element when evaluated in a single-section filter prototype, operated satisfactorily with respect to tunability and selectivity. However, due to the circuit unsymmetries between terminal x-z and y-z, the observed responses were dependent on the direction of the power flow. With the gate and varactor voltages adjusted vs. frequency, as shown in Figure 11, the element could be tuned to the frequencies shown with 0-dB transmission loss independent of power flow direction. The return loss in the forward and reverse direction for the same settings, as shown in Figure 12, was noticably different as was the 3 dB bandwidth, as shown in Figure 13. These unsymmetric responses could be compensated by changing the loading at one port of a single-section filter. Even in a two-section arrangement the two elements can be mounted back-to-back (terminal y of the first element facing terminal x of the second element) maintaining electrical symmetry. However, in any odd-numbered section filter, symmetry is absent leading to coupling difficulties and unsymmetric responses.

A new symmetric element was designed and fabricated on a 5 x 5 x .635 mm alumina substrate. The element contains two FET's, two varactors, and in printed circuit form, all necessary chokes. The symmetric electrical configuration, as shown in the equivalent circuit of Figure 14, should assure nearly bilateral performance in multisection filters. The element is mounted on a .25 mm thick copper plate that holds bypass capacitors and protective resistors for the gates of the FET's and the varactors. Figure 15 shows a photograph of such an element. Initial evaluation of one element showed good tunable performance over the 9.1 to 9.6 GHz frequency band with varactor voltages ranging between 10 and 25 volts. Spurious oscillations observed at 4 GHz and 15 GHz were caused by the RF choking circuitry and were suppressed by resistive loading of the chokes. A low-Q, non-tunable resonance near 11 GHz is created by the physical discontinuities at the edges of the element which caused spurious transmission near this frequency in a single-section filter. An element voltage-tuned for 0-dB transmission loss at frequencies as shown in Fig 16 gave essentially equal performance with respect to selectivity and matching when the power flow was reversed. Figure 17 shows the observed VSWR and Fig. 18 the bandwidth for both forward and reverse power flow. A total

of twelve such elements were fabricated during the course of this program which were used in preliminary testing and in the construction of the final hardware.

3. Element Evaluation

Single-section performance of an unsymmetric resonant element, as shown in Figure 10, was evaluated in detail. The element and the $\lambda/4$ matching transformers were mounted in a 32 x 22 x 13 mm brass housing, as shown in Figure 19. The effects of temperature and drive level were also investigated on this structure. The element was adjusted to operate over the 6.4 to 7.7 GHz frequency. The measured performance characteristic, as plotted in Figure 20, shows the varactor voltage required as a function of frequency setting, also shown is the gate voltage at each frequency to maintain zero dB transmission loss and the observed 3 dB bandwidth at each of the settings. Taking advantage of the full tuning range of the varactor, a frequency band of 1500 MHz could be covered. This observed tuning range is in good agreement with the calculated range of 1800 MHz using the FET model and estimated circuit parameters of carrier interconnections and varactors.

The plot in Figure 21 shows the relationship between input power and output power with the filter adjusted for 0 dB transmission loss and a varactor voltage of 25 volts. The observed characteristic is linear up to input power levels of -5 dBm.

Temperature effects, as observed over the 10°C to 50°C range, are shown in Figure 22. With the operating voltages (drain, gate, and varactor) kept constant, the center frequency decreased by 900 kHz/°C, the midband transmission decreases by 0.3 dB/°C, and the 3 dB bandwidth increases by 800 kHz/°C. When the center frequency (F_o = 7.125 GHz) and the midband loss (0 dB) were kept constant, as shown in Figure 23, a varactor voltage and gate voltage increase of approximately 20 mV/°C were necessary to compensate the effects of temperature, whereas the 3 dB bandwidth remained essentially constant over the observed temperature range.

Tuning speed evaluation was attempted by driving the varactor of the filter by a programmable two-level power supply. The lower level was set at 2 volts and the upper level at 10 volts. These levels were switched at 100 µs intervals. The settling time, determined by the D/A converter used in the power supply, is about 5 µs. The input waveform to the varactor and the detected power output of the filter was monitored on an oscilloscope. The

input frequency was set to correspond to the high varactor voltage setting. In the photographic sequence of Figure 24 a, b, and c, the input waveform (lower trace) to the varactor and the detected power output (upper trace) are shown for the time scales/division of 20 μs, 2 μs, and .5 μs, respectively. Even though the true speed capability of the filter is masked partially by the RF-filtering and by the power supply ringing, judging from Figure 24 c, the detected output lags at most by 200 ns. From this test it can in inferred that speed limitations, as expected, will be mainly a function of external parameters (filtering, driver impedance, etc.), rather than of device parameters (FET, varactors).

4. Coupling of Elements

The operation and design of coupled resonator filter is well described in Reference 3. For this program the procedures described there are applicable for attaining approximate maximally flat responses. As long as the resonator elements are essentially in lumped form, band-pass filters constructed with them have basically no additional pass bands at higher frequencies. A band pass filter arrangement realizable at microwave frequencies, is shown in Figure 25. A number of resonators, X, and inverters, K, are alternately connected so as to produce the desired filter response. The resonators are represented by the reactance function $X(\omega)$. The inverters are basically impedance transformers that provide an image phase in odd multiples of ±90°. The two end-inverters could provide transformation only.

The resonator is adequately described by its reactance slope parameter, S, and its internal losses, R_x, at the resonant frequency, ω_o. The S and Q_o of the resonator are given by

$$S = \frac{\omega_o}{2} \left. \frac{dX}{d\omega} \right|_{\omega_o} \text{[ohm]}$$

$$Q_o = \frac{S}{R_x}$$

The shape of the filter response is determined by specifying the proper value of impedance-inverter parameter K. The K of the end-sections can be expressed as:

$$K = \left(\frac{R_o \, Q_o \, R_x}{Q_e} \right)^{\frac{1}{2}} = \left(\frac{R_o \, S}{Q_e} \right)^{\frac{1}{2}} = \left(R_o \, R_e \right)^{\frac{1}{2}}$$

in which Q_e is the according to the desired selectivity chosen external Q of the arrangement. The inverter parameter for the center section, K', depends upon the coupling factor, c, such that,

$$K' = cS$$

In the case of critical coupling which gives single peak responses with minimum midband loss,

$$K' = \frac{S}{Q_e} + \frac{S}{Q_o} = R_e + R_x$$

in which R_e is the external resistance reflected into the resonator. Values of K' smaller or larger as given above, give under-coupled or over-coupled responses, respectively.

The major inverter and matching network used during this program are depicted in Figure 26. Two types of end matching networks were used, one a quarter wave-length transmission line (Figure 26 a) that transforms the 50 ohm terminations R_o to:

$$R_x = Z_o^2/R_o$$

and in which Z_o is the transformer impedance; and the other a capacitive matching network (Figure 26 b) that in addition to the real transformation R_x reflects a series capacitance C_x into the resonator's proper. This additional reactance has to be taken care of in the filter design. In the two and three-section filter experiments the capacitive inverter, as shown in Figure 26c, was used. The negative capacitances are absorbed into the adjacent positive elements of the resonators. In addition to the difficulties to realize this idealized inverters at microwave frequencies parasitic coupling within the filter enclosure pose a problem. As described in subsequent section, metallic partions were used to prevent the effects of the undesired coupling.

SECTION III

EXPERIMENTAL RESULTS

1. Two-Section Filter

In the mid-period of this program it was realized that with the delivery of two three-section filters at the end of the program the unresolved problem of tuning voltage tracking and voltage addressing as a function of desired frequency between the individual filter sections would delay systems applications. It was, therefore, decided to fabricate a two-section filter with four accessible tuning voltages that would enable NRL to perform preliminary tracking and addressing experiments.

A two-section filter with two symmetric resonant elements, as described in Section II-2, was constructed and housed in a 48 x 32 x 16 mm brass enclosure. The photograph of Figure 27 shows the details of the construction. The two elements are capacitively coupled via a 17 pF MOM-capacitor located between the elements. Two short 50-ohm microstrip transmission line sections on alumina provide matching and connections between input and output and the respective elements. Six terminal-type feed-through capacitors give access to the necessary DC operating voltages. A metallic partition, not shown in the photograph, prevents parasitic coupling between the elements and avoids a cavity type resonance otherwise introduced by the metallic enclosure.

Individual elements were tested and adjusted to operate in the 9.1 to 9.6 GHz frequency range prior to assembly. In the final assembly the tuning range was, however, limited by the reactive loading of the coupling capacitor and parasitics of the bias circuitry within the enclosure. It is for this reason that the tuning range of the filter covered the 8.2 to 9.0 GHz frequency range. The purpose of this preliminary two-section filter was to provide valuable tuning voltage data, therefore, no additional effort was made to correct the tuning frequency range to the desired 9.1 to 9.6 GHz range before delivery.

The necessary four voltages of the final filter, as evaluated at each frequency, are listed in Table I for a midband loss of 0 dB. The power input was maintained at a level of 10 μW, the drain-source voltage was 6 volts, and the case temperature 23°C. The respective plots of Figures 28, 29 and 30 show the two gate voltages, the two varactor voltages, and 3 dB bandwidth, all vs.

TABLE I. TWO-SECTION FILTER

F (GHz)	VV1 (V)	VV2 (V)	VG1 (V)	VG2 (V)	ID (MA)	BW (MHZ)
8.280	2.5	4.37	2.80	3.07	45.7	60
8.360	3.0	5.16	2.87	3.07	41.7	65
8.439	3.5	5.74	2.88	3.21	37.9	65
8.500	4.0	6.35	2.90	3.28	35.1	65
8.550	4.5	7.00	2.94	3.40	30.9	62
8.590	5.0	7.64	2.95	3.43	30.1	65
8.699	6.0	8.76	3.00	3.54	26.3	65
8.785	7.0	10.06	3.05	3.63	23.5	65
8.850	8.0	11.25	3.11	3.68	21.5	60
8.910	9.0	12.65	3.13	3.74	20.2	65
8.975	10.0	13.77	3.17	3.79	18.7	55

VD=6-VOLT
PIN=10-μW
C=0-DB
T=23° C

frequency. The transmission responses as measured on an automatic network analyzer for four distinct adjustments, as listed in Table I, are shown in Figures 31 through 34. The responses are close to those ideally expected from a two-section coupled resonator filter. The response shapes, however, are different for different frequency settings as is evident from the shown response plots. The filter was delivered to NRL after evaluation.

2. Three-Section Filter

The final three-section filters each contain three-symmetric resonant elements (Section II-2). The three elements are capacitively coupled and end-loaded via two 50-ohm alumina microstrip lines. The filter is enclosed in a 55 x 32 x 17 mm brass enclosure with SMA connectors providing RF input and output; capacitive type feedthrough give external access to the DC connections of the varactors and the FETs of the three elements. Metallic partitions between each adjacent element prevent RF stray coupling between elements. The

photograph in Figure 33 shows the construction with the partitions in place. Figure 34 shows a closer detail of the filter near the resonant elements with the partitions removed.

Each resonant element was individually adjusted to operate in the 9.1 to 9.6 GHz frequency range. Elements were also tested in pairs using special test structures before assembly in each of the final filter structures. Some retuning was required because of additional reactive loading by the coupling circuitry. Initial tests showed, as described below, that the resonant frequency range for each element was further reduced when all three elements were interconnected. The lowering of the tuning frequency range is caused by the reactive effects of coupling and bias networks, and distributed element carrier resonances near the upper frequency range. This frequency shift in multiple element filters requires single resonator tuning adjustments to accordingly higher frequencies.

The first assembled unit was evaluated at room temperature and with the drain voltage at 6 volts. The RF drive level was kept constant at 10 μW at each frequency and the transmission loss was maintained to 0 dB with the gate voltages, while the varactor voltages were adjusted to give the best response at each of these frequencies. Table II lists the six voltages that gave the best results at the frequencies listed. The plot in Figures 37 and 38 show the gate voltages and varactor voltages, respectively, both vs. frequency. The 3 dB bandwidth, which varied between 60 and 75 MHz over the 8.4 to 9.2 GHz tuning range, is shown in Figure 39. The next three figures (Nos. 40, 41, and 42) show individual transmission responses at three distinct frequencies. The tuning frequency range of this unit 1 fell short of the desired range from 9.1 to 9.6 GHz; however, it was agreed upon to omit necessary corrective changes in order not to jeopardize the survival of the entire filter.

The elements of the second unit were adjusted at some higher frequency from the beginning so as to take the loading effects observed on the first unit into account. Except for the special care taken in the element adjustment, the construction of unit 2 is identical to unit 1. After assembly and final tuning adjustments, the filter was evaluated at room temperature and with a drain voltage of 6 volts. Table III lists the voltage settings for some select frequencies in the 9.0 to 9.6 GHz tuning band. The adjustments are those representative of the best three-section response with a midband transmission loss of 1 dB and a RF drive level at 10 μW. It can be noted that

TABLE II. THREE-SECTION FILTER (UNIT #1)

F (MHZ)	VV1 (V)	VV2 (V)	VV3 (V)	VG1 (V)	VG2 (V)	VG3 (V)
8450	2.13	2.07	3.00	2.42	3.10	3.33
8570	3.04	2.41	3.09	2.27	3.26	3.28
8750	4.47	3.62	4.90	2.47	3.31	3.06
8870	5.83	4.94	5.50	2.47	3.26	3.59
8930	6.48	5.49	6.53	2.42	3.27	3.53
8940	6.89	5.82	6.97	2.42	3.23	3.37
8980	7.53	6.38	7.61	2.50	3.16	3.73
9000	8.07	6.72	8.33	2.50	3.16	3.73
9080	9.75	7.68	9.41	2.49	3.16	3.73
9120	11.32	8.24	11.14	2.46	3.14	3.50
9185	15.41	9.22	16.72	2.36	3.08	3.56
9210	19.50	10.00	21.30	2.33	3.00	3.48

CAIN=0DB

PIN=10UW

VD=6VOLT

T=23 C

gate voltages 2 and 3 were constant over the tuning range, a desirable but not necessary condition. Plots of gate voltage and varactor voltage vs. frequency are shown in Figures 43 and 44, respectively. Figure 45 depicts the observed 3 dB bandwidth. The responses at six frequencies in the band are shown in Figures 46 through 52. The response shapes are varying but are representative of the filter and can be altered with adjustments of some or all of the gate and varactor voltages. The measured noise figure vs. frequency varies between 20 and 24 dB, as shown in Figure 53. The dependence of transmission loss as a function of drive level is shown in Figure 54. At 9.1 GHz and drive levels below -20 dBm, output levels were found to be linear; at an input level of -10 dBm the loss increases by 3 dB.

TABLE III. THREE-SECTION FILTER (UNIT #2)

F (MHZ)	VV1 (V)	VV2 (V)	VV3 (V)	VG1 (V)	VG2 (V)	VG3 (V)
9000	1.80	2.10	1.10	2.49	2.79	3.82
9100	2.10	3.50	1.68	2.36	2.79	3.82
9200	2.60	5.90	2.12	2.21	2.79	3.82
9300	3.10	9.00	2.60	2.07	2.79	3.82
9400	4.50	12.20	3.34	1.93	2.79	3.82
9500	6.10	16.20	4.00	1.80	2.79	3.82
9600	9.10	19.10	5.00	1.62	2.79	3.82

GAIN=-1DB

PIN=10UW

VD=6VOLT

T=23 C

Temperature effects over the 20°C to 35°C range, with the filter tuned to 9.1 GHz, are plotted in Figures 55 through 58. The 3 dB bandwidth decreases monotonically at a rate of 1.33 MHz/°C, the midband transmission decreases at a rate of .67 dB/°C, the rejection at twice the 3 dB bandwidth decreases at a rate of .4 dB/°C, and the total drain current decreases at a rate of .4 mA/°C.

SECTION IV

CONCLUSIONS AND RECOMMENDATIONS

The Phase II, Task 1 program achievements, findings, and recommendations can be summarized as follows:

- The tunable resonant element developed during Phase I was successfully redesigned into a planar form that is more amenable to multisection filter design. This element was also realized in symmetrical form in a 5 x 5 x 1 mm size with all necessary RF-chokes printed on the substrate.
- A preliminary two-section filter for tracking and addressing experiments by NRL was constructed, tested, and delivered. This filter tunes from 8.2 to 9.0 GHz with a 3 dB bandwidth ranging between 60 and 70 MHz.
- Two three-section filters, each housed in a 55 x 32 x 17 mm enclosure, were constructed, tested, and delivered. One of these filters covers the desired 9.1 to 9.6 GHz frequency range and meets the other electrical and physical requirements, except the 3 dB bandwidth which extends from 80 to 120 MHz within the tuning band.
- The tuning bandwidth is presently limited by the reactances of the coupling and loading networks which effectively reduced the capacitive ratio of the tuning varactors. To a minor degree, the bandwidth is also limited by the effective bandwidth of the coupling and loading networks.
- The upper tuning frequency is presently limited by a carrier resonance near 11 GHz that interferes with the normal tuning characteristic of the resonant element at frequencies above 9.8 GHz.
- The 3 dB bandwidth is limited by the actual coupling and loading, together with the maximum gate voltage that ensures stability.
- Temperature effects observed lead to the belief that oven controlled operation will be necessary in most systems applications.

- Seve · stability problems encountered in the final stages of the program were traced to FET fabrication changes and high-Q RFchokes. The FET problem was resolved by the FET supplier making available devices with characteristics close to those of earlier devices. Resistive loading of the chokes also eased the stability problem.
- Metallic partition introduced between resonant elements allow slight correction of the otherwise fixed coupling between elements and small response adjustment.
- Power level sensitivity increases with the number of elements within the filter and is related to the degree of stability. Adjustments too close to potential instabilities lead to drive-level sensitive performance.
- In order to meet realistic tuning accuracy and resettability requirements, the case temperature has to be maintained within ±2°C, the controllable varactor voltages to within ±10 mV, and the gate voltages to within ±5 mV.
- Tuning speed is mainly determined by the supply impedance and the EMI filtering. The prototype filters are limited to a speed of about 10 µs by these components. Ultimate speeds as low as 30 ns are possible with 100 pF feedthrough capacitors and 200 ohm protective resistors.
- The 55 x 32 x 17 mm size of the filter represents an oversize enclosure selected for construction conveniences only. A 40 x 32 x 17 mm enclosure would have been sufficient. The actual weight of 175 g entails a solid brass structure. Using aluminum, the weight scales to 58 grams.
- Future tasks should concentrate to extend the upper frequency range of operation, to reduce tuning range limiting factors to a minimum, improve coupling circuitry to a poin' at which selectivity can be better controlled, and to select a suitable temperature range for oven control.

SECTION V

REFERENCES

1. A. Presser, "Ultra-Fast Tunable Microwave Filter," Final Report Contract No. N00173-77-C-0201, August, 1978.

2. P. Wolf, "Microwave Properties of Schottky-Barrier Field-Effect Transistors," IBM Journal of Research Development, March, 1970.

3. G. L. Matthaei, et al., "Microwave Filters, Impedance-Matching Networks and Coupling Structures," McGraw-Hill Book Company, 1964.

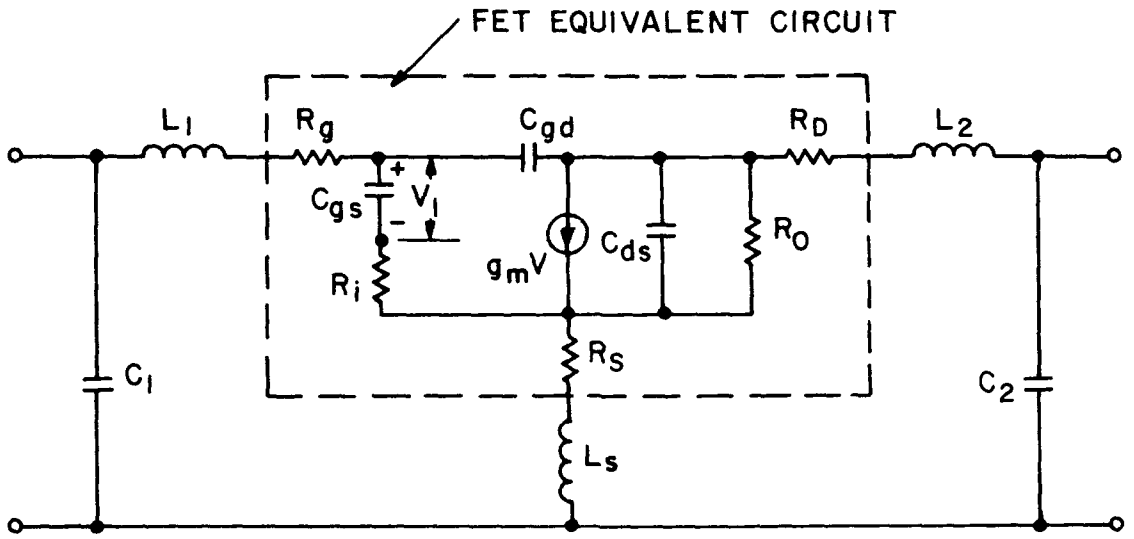

Figure 1. Equivalent circuit of FET.

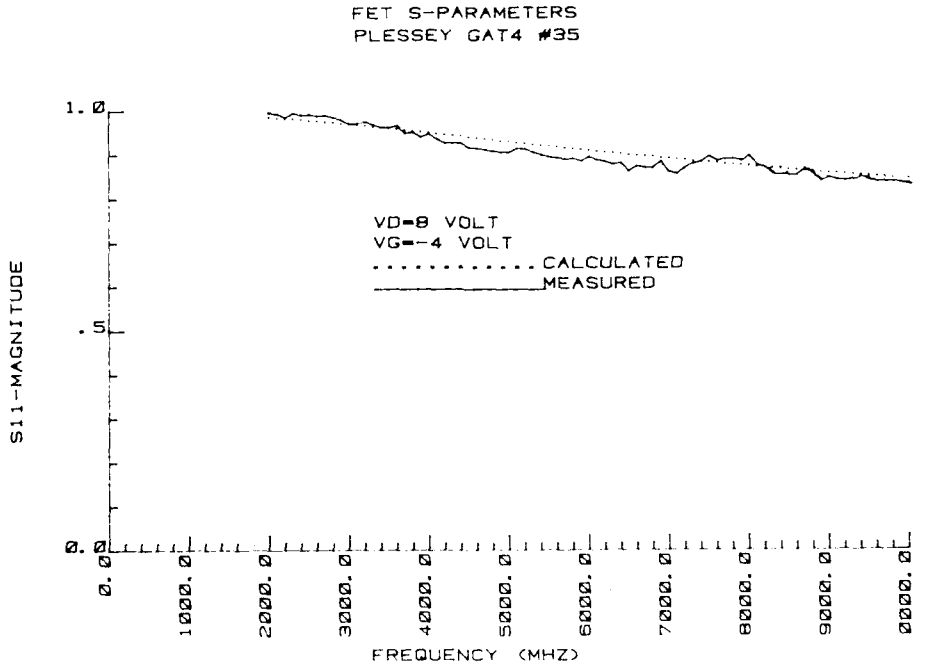

Figure 2. S_{11} mag vs. frequency.

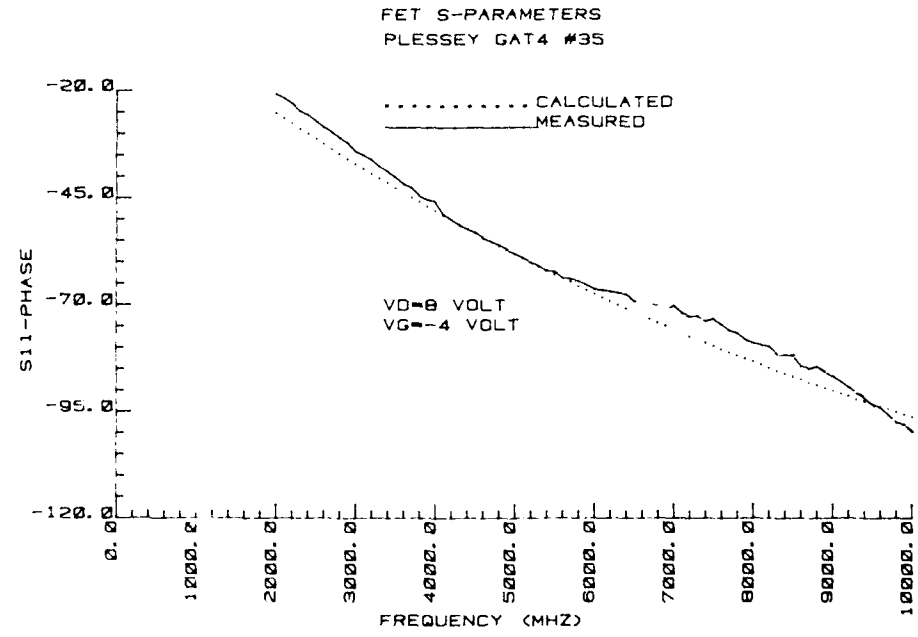

Figure 3. S_{11} angle vs. frequency.

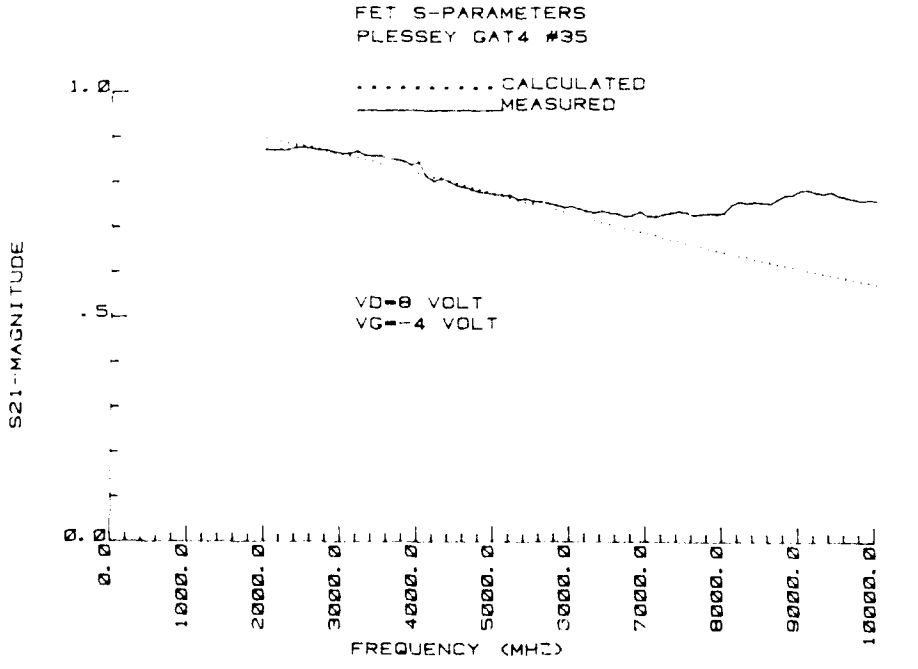

Figure 4. S_{21} mag. vs. frequency.

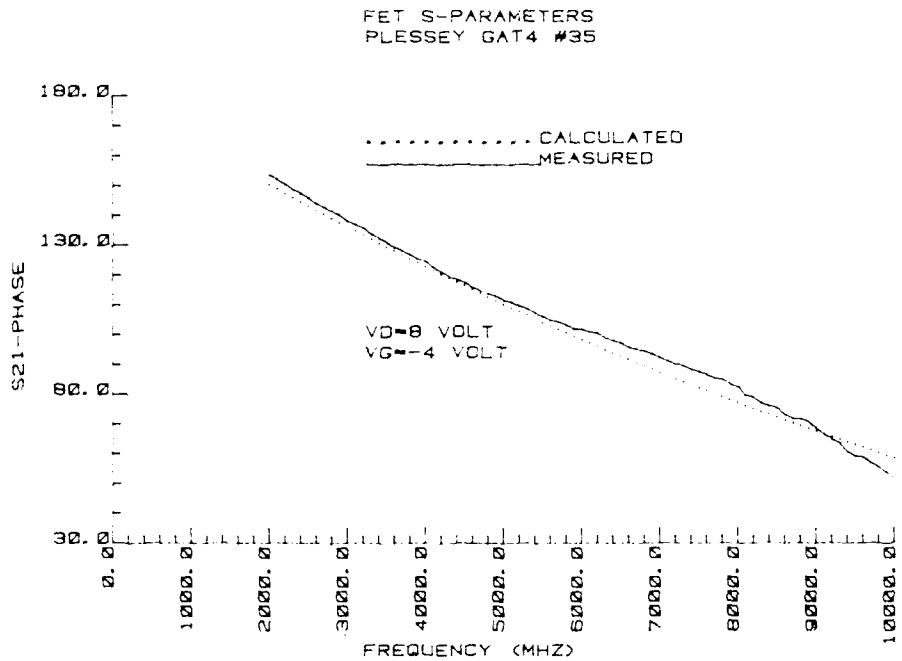

Figure 5. S_{21} angle vs. frequency.

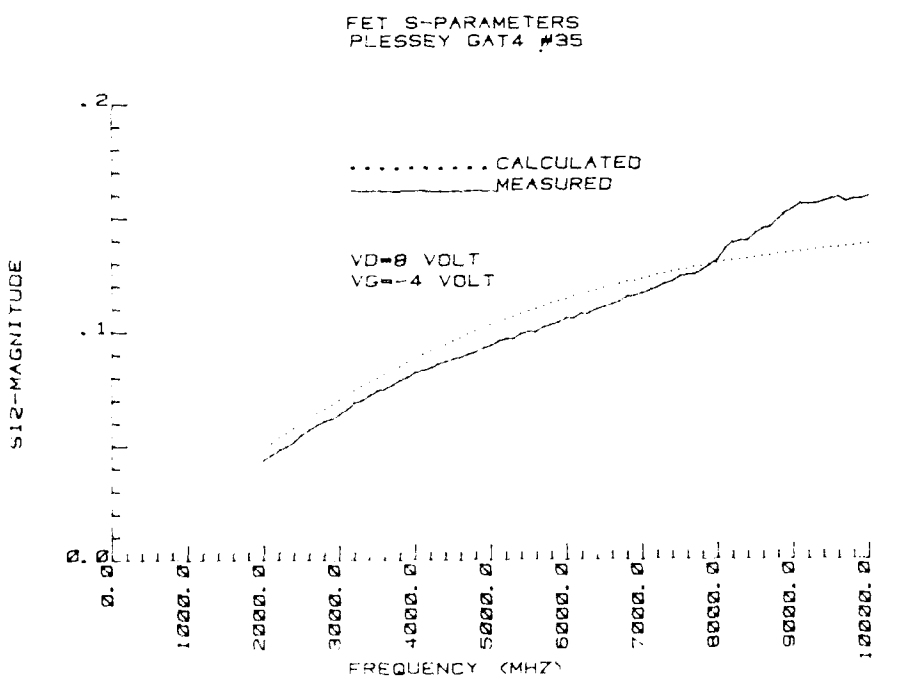

Figure 6. S_{12} mag. vs. frequency.

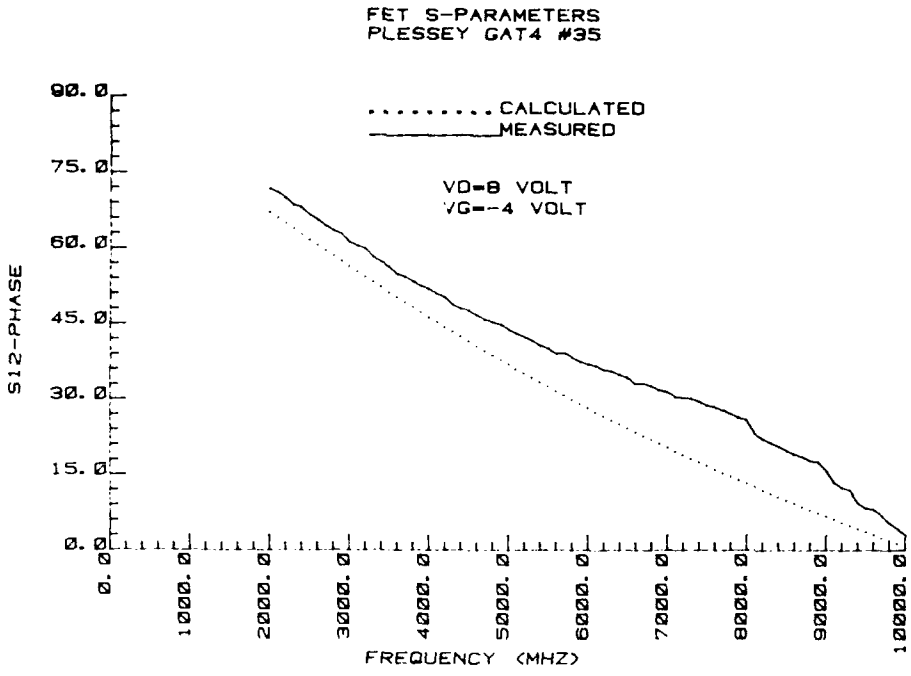

Figure 7. S_{12} angle vs. frequency.

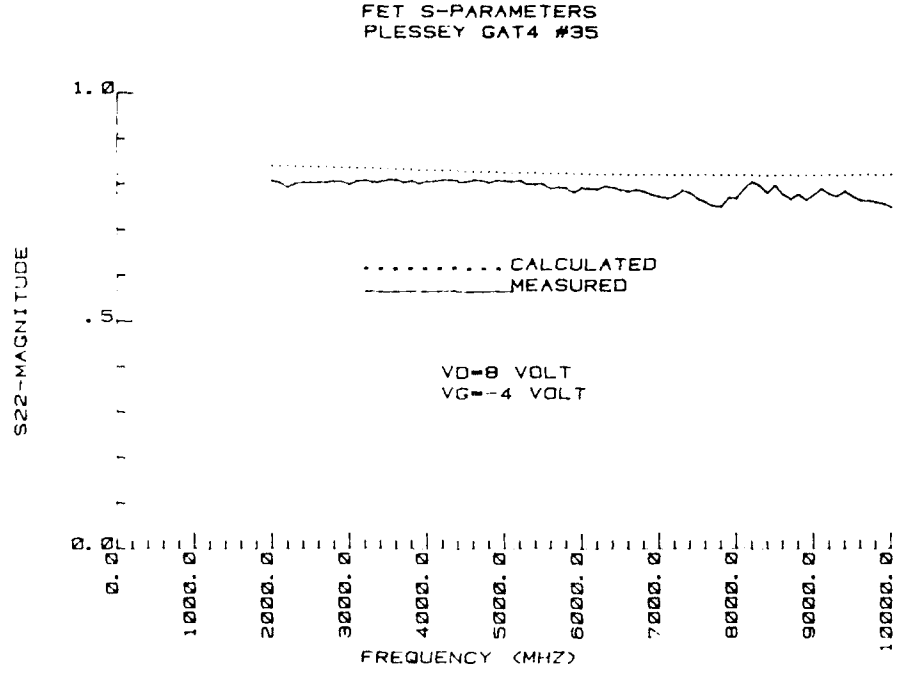

Figure 8. S_{22} mag. vs. frequency.

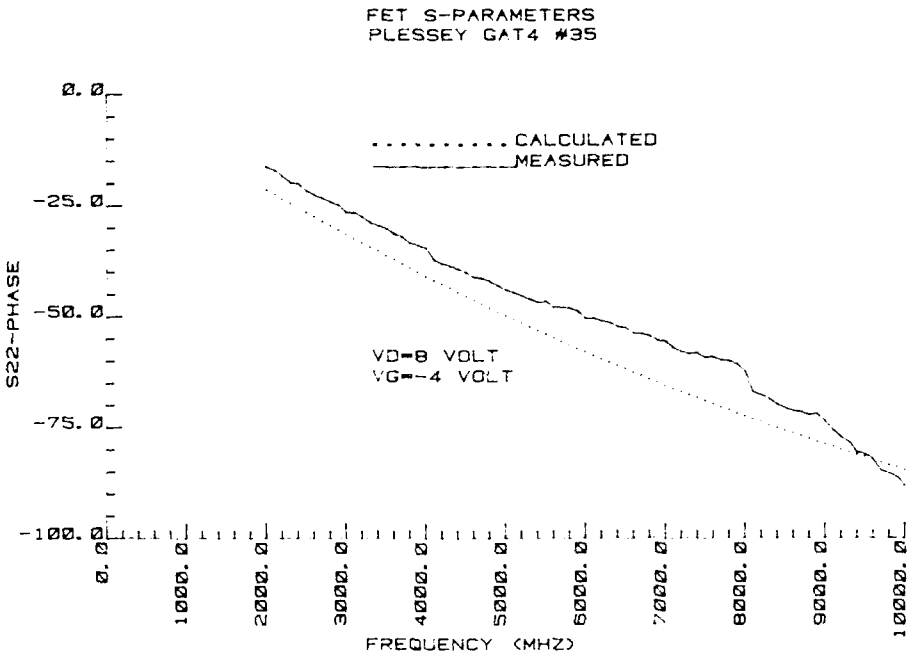

Figure 9. S_{22} angle vs. frequency.

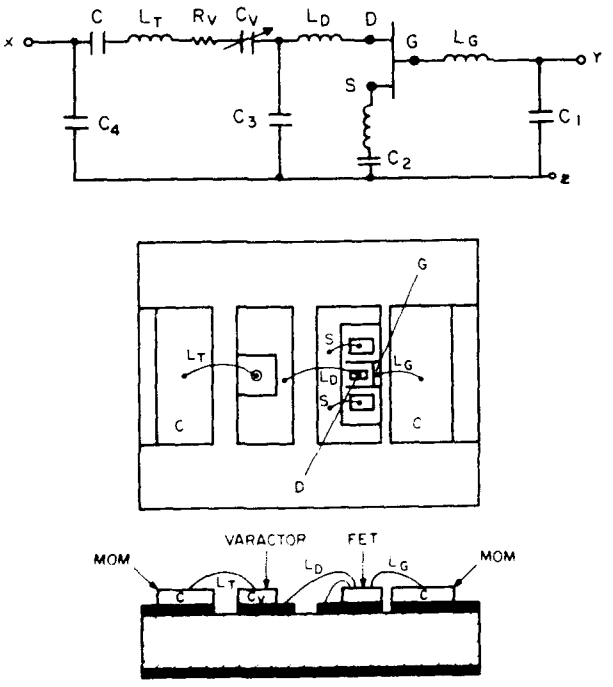

Figure 10. Planar resonant element (unsymmetric).

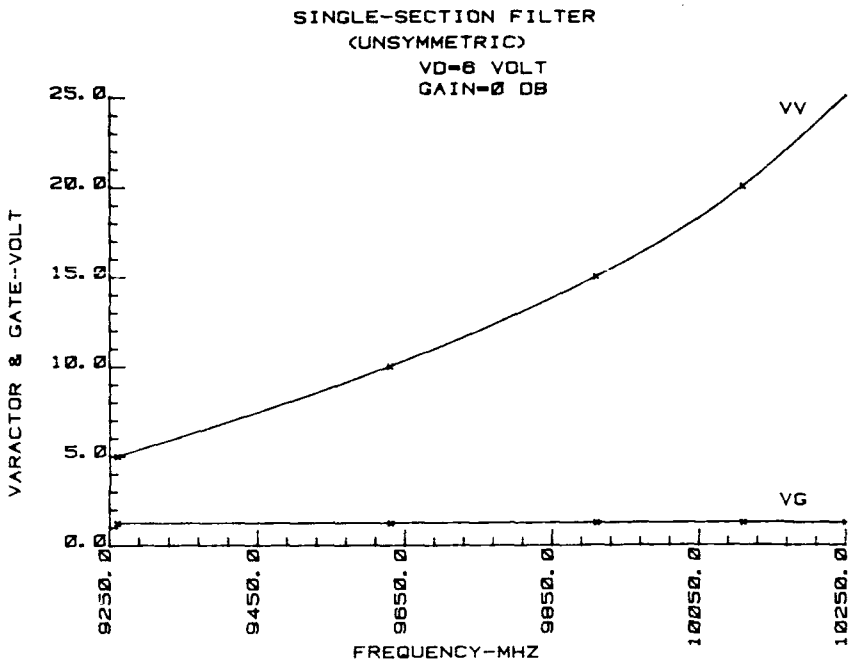

Figure 11. Varactor and gate voltage vs. frequency (unsymmetric).

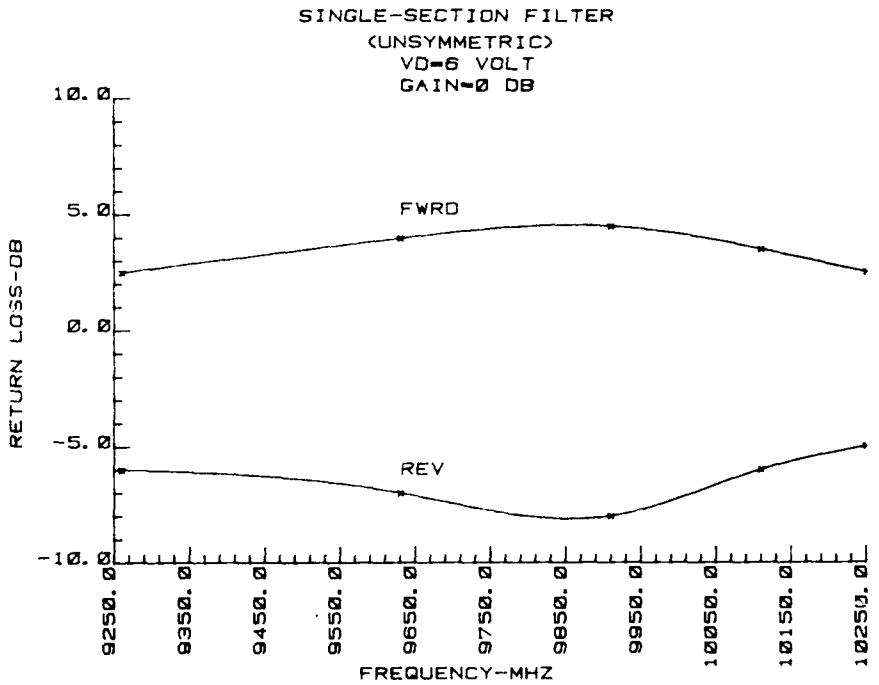

Figure 12. Forward and reverse return loss (unsymmetric).

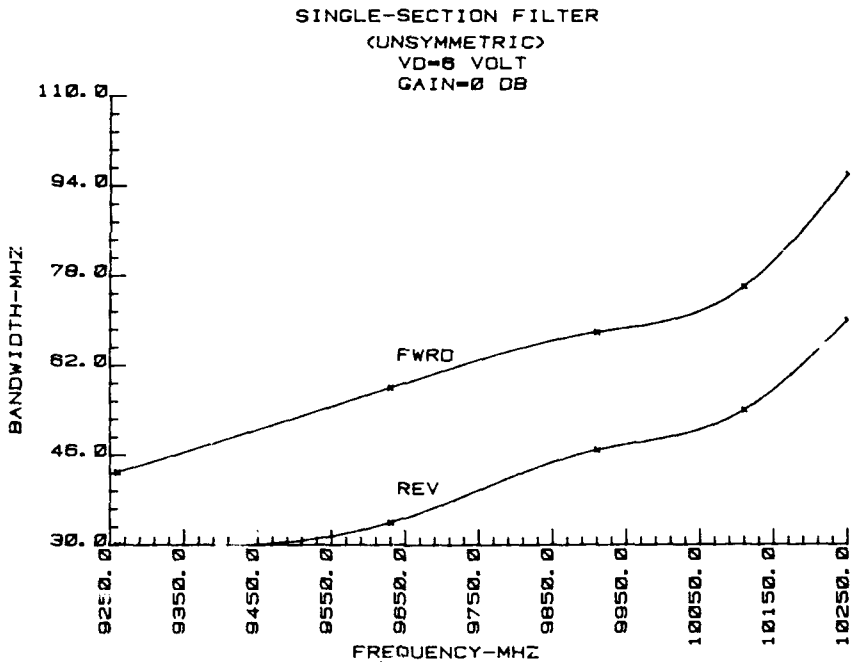

Figure 13. Forward and reverse 3 dB bandwidth (unsymmetric).

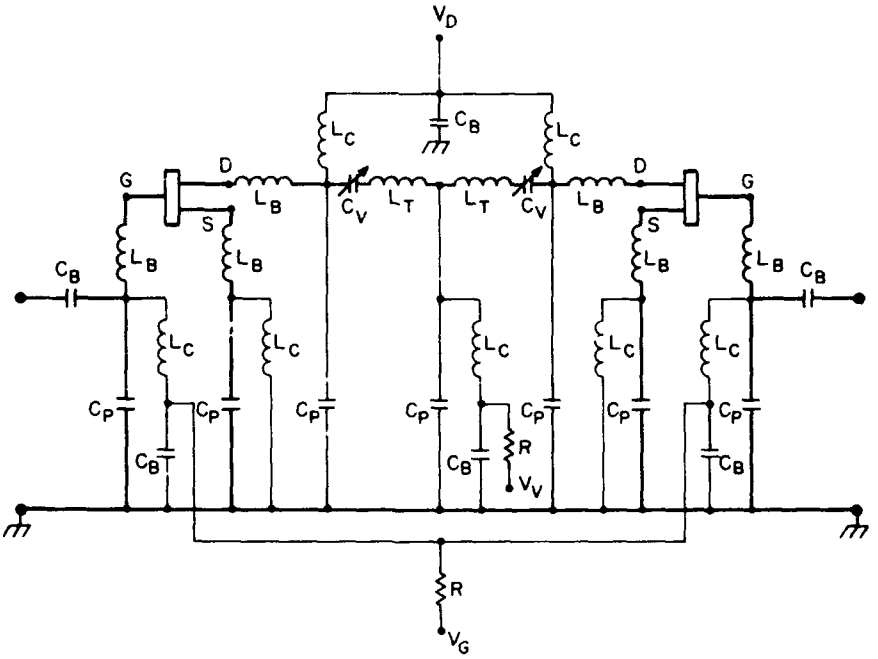

Figure 14. Equivalent circuit of symmetric element.

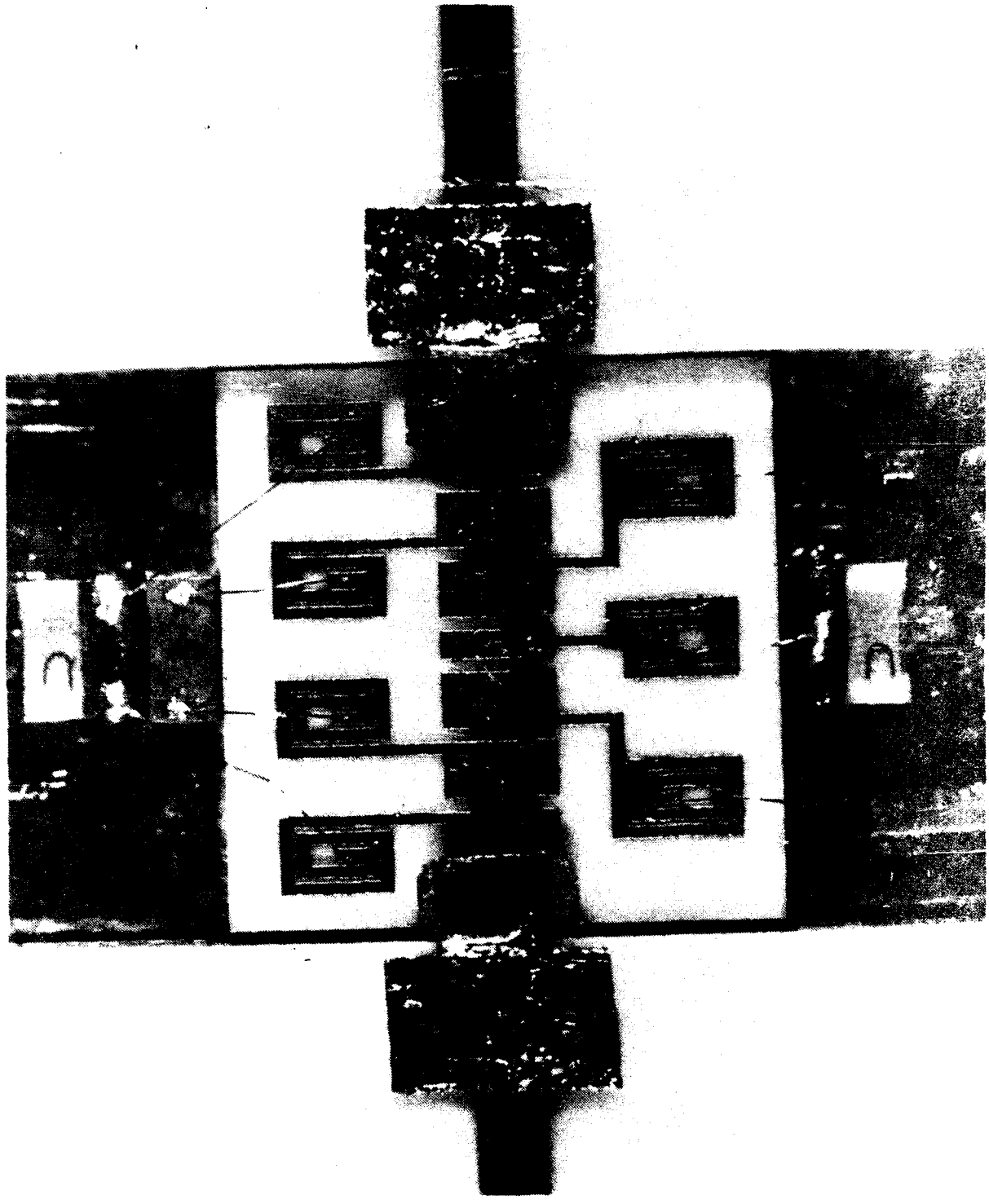

Figure 15. Planar resonant element (Symmetric).

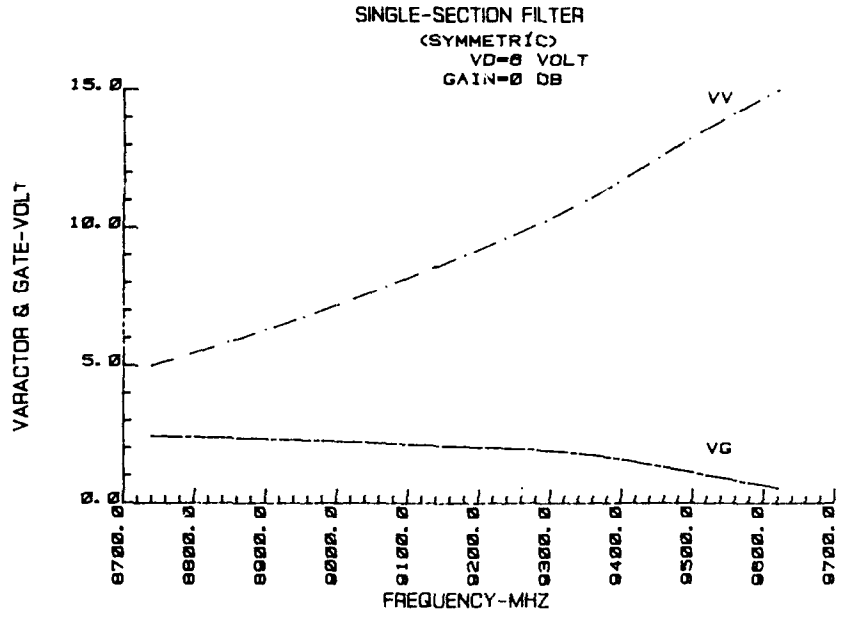

Figure 16. Vararactor and gate voltage vs. frequency (symmetric).

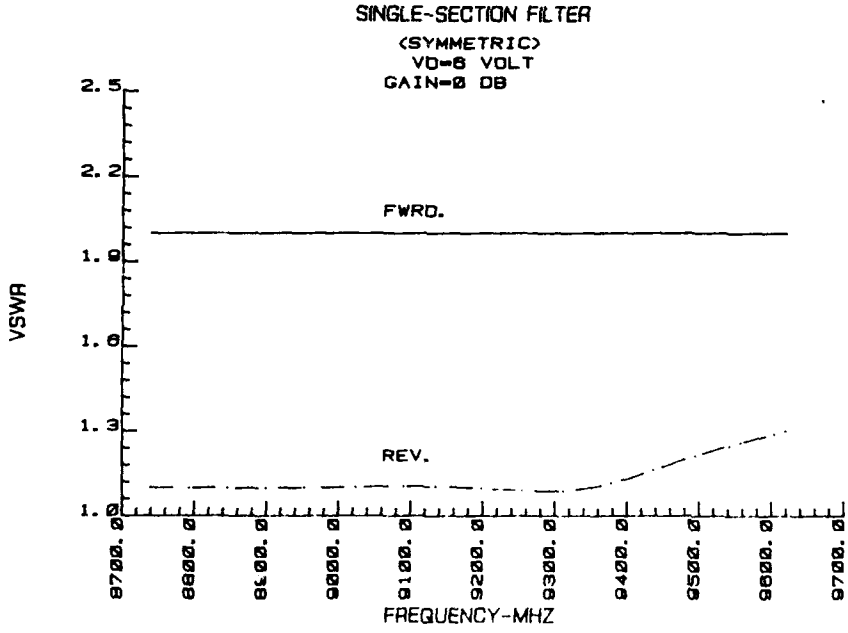

Figure 17. Forward and reverse VSWR vs. frequency (symmetric)

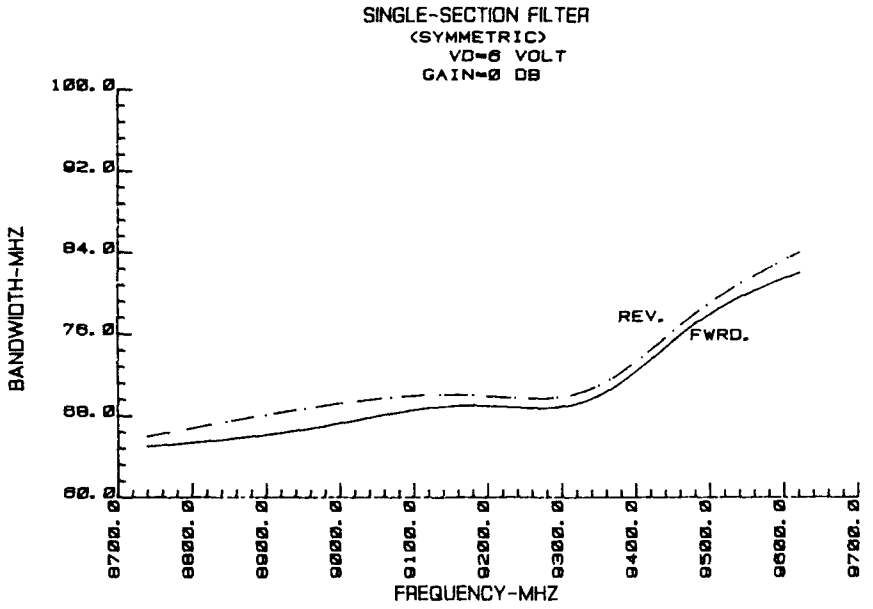

Figure 18. Forward and reverse third bandwidth vs. frequency (symmetric).

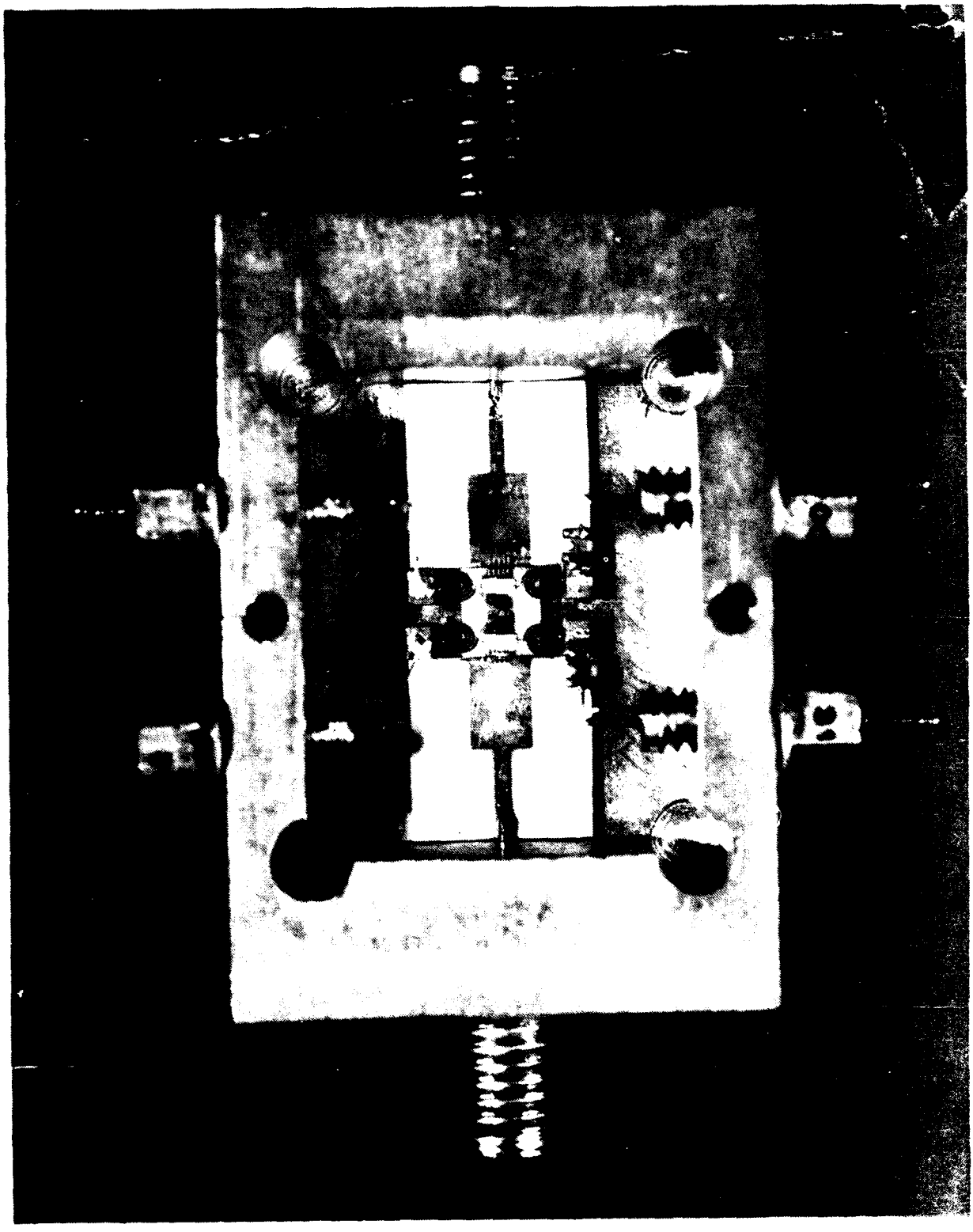

Figure 19. Single-section test filter.

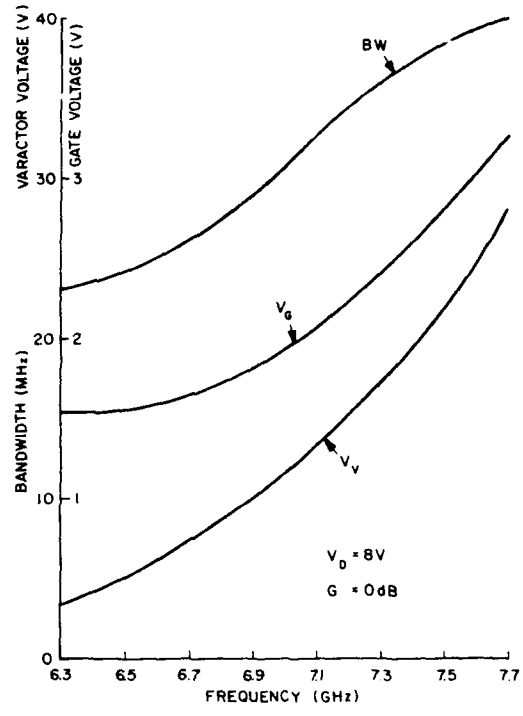

Figure 20. Single-section filter performance.

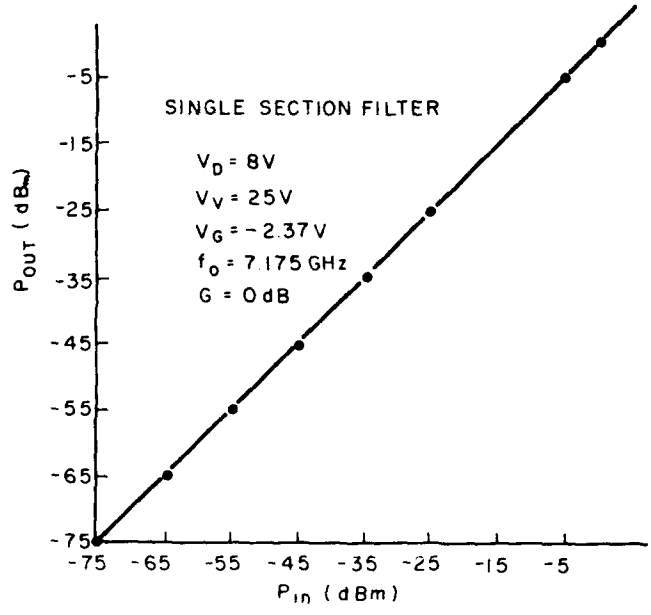

Figure 21. P_{out} vs. P_{in} characteristics.

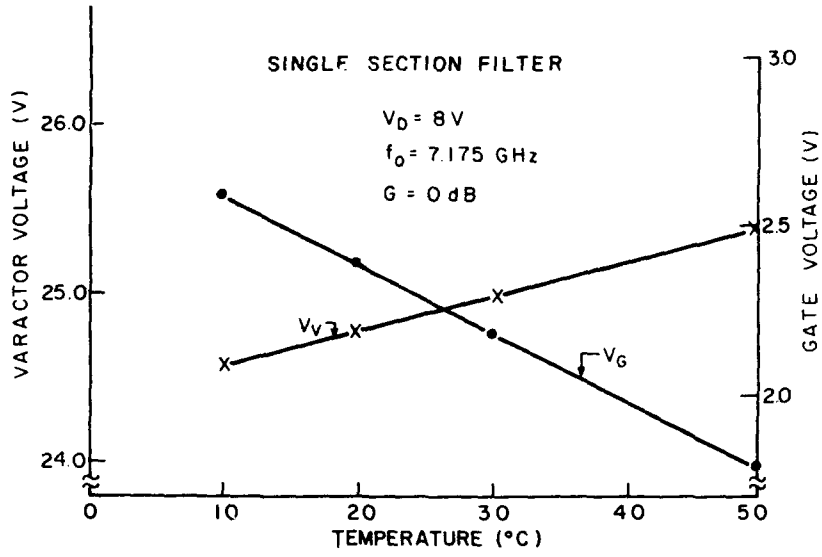

Figure 22. Temperature effects (single-section).

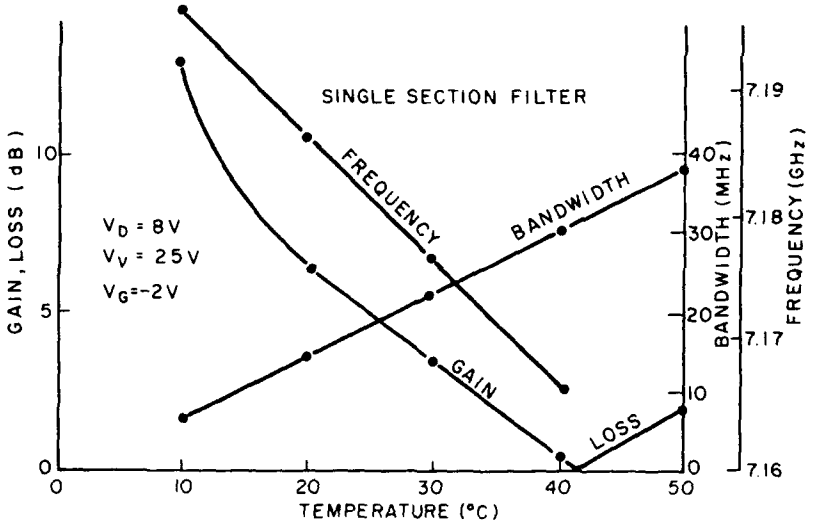

Figure 23. Temperature compensation (single-section).

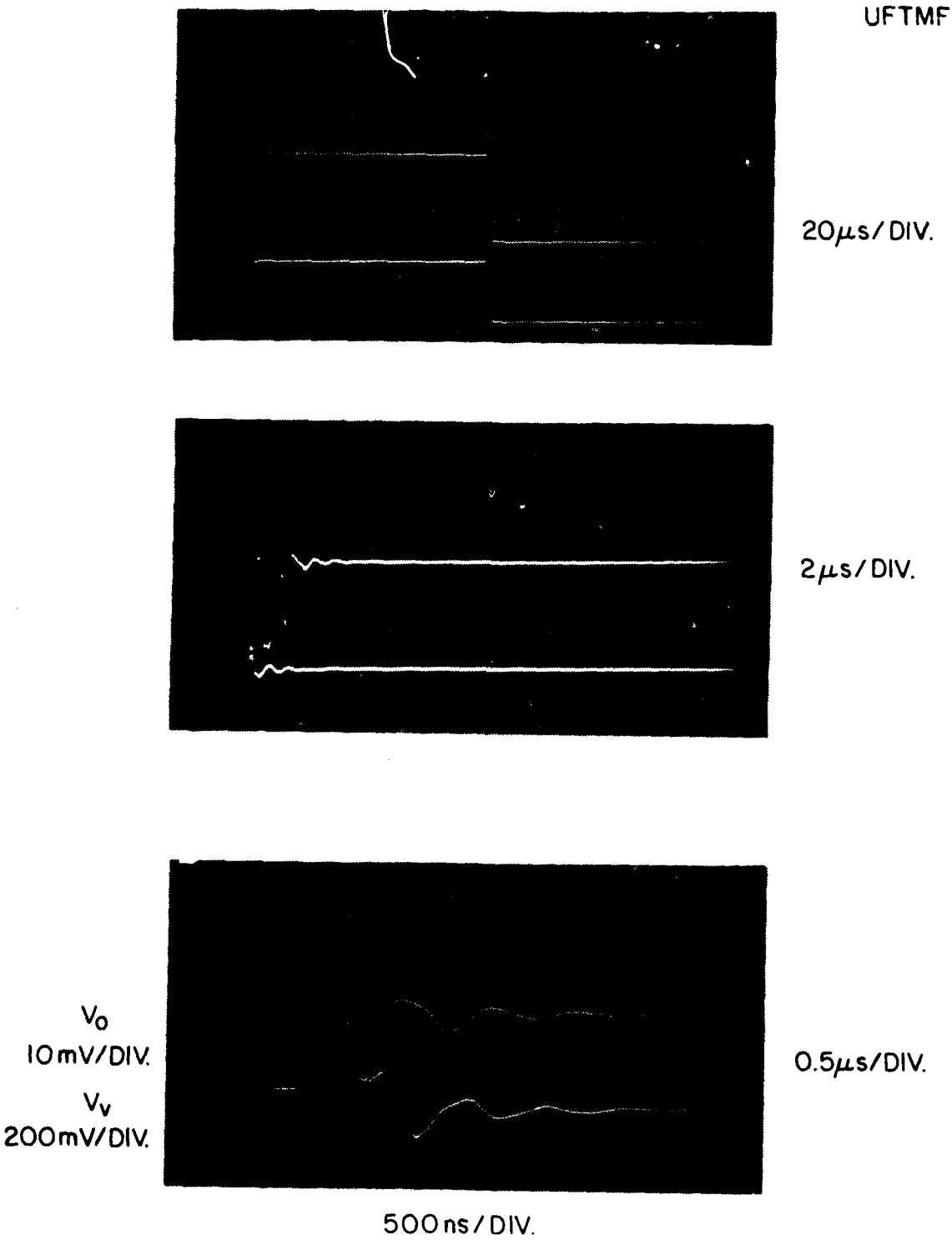

Figure 24. Switched tuning characteristic.

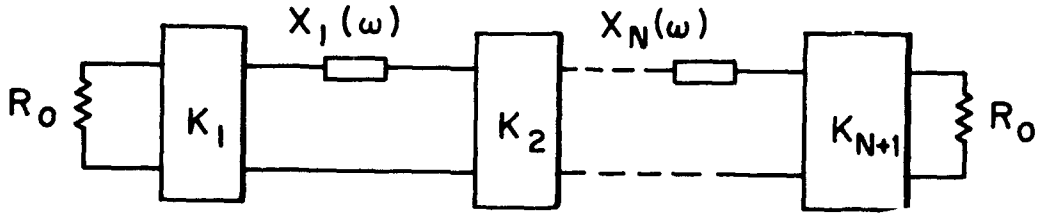

Figure 25. Multisection filter diagram.

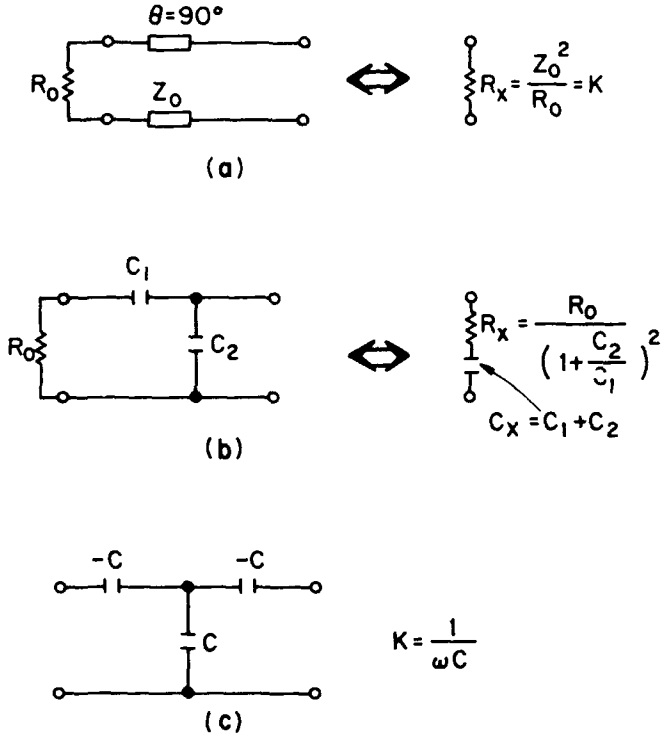

Figure 26. Inverter and matching networks.

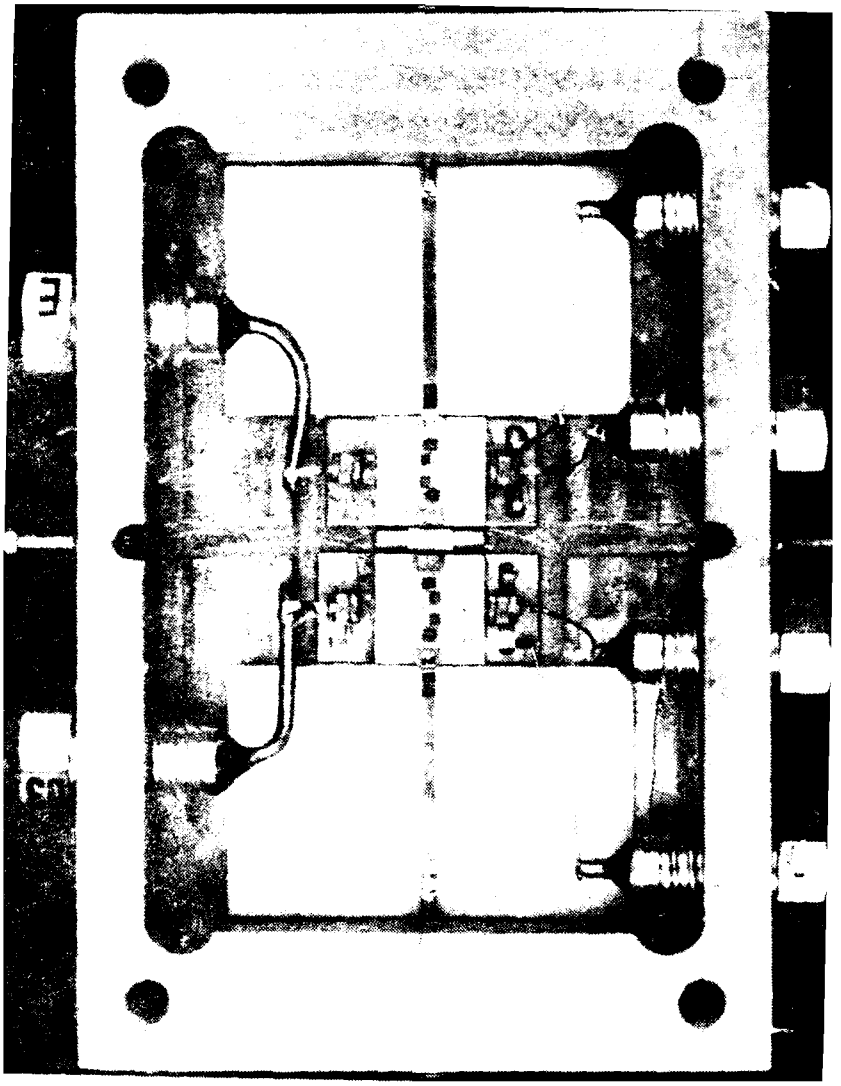

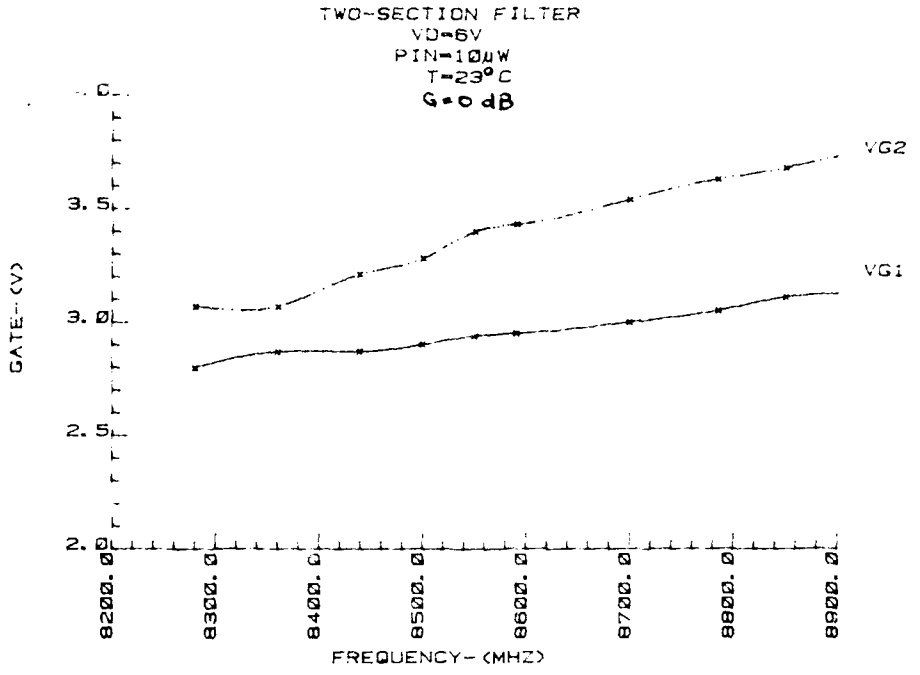

Figure 28. Gate voltage vs. frequency (two-section).

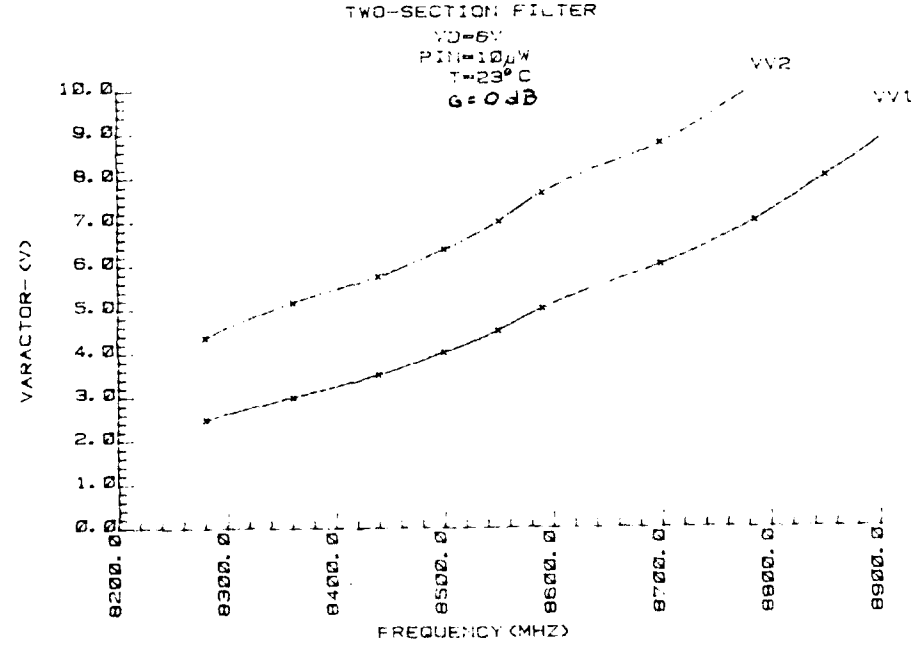

Figure 29. Varactor voltage vs. frequency (two-section).

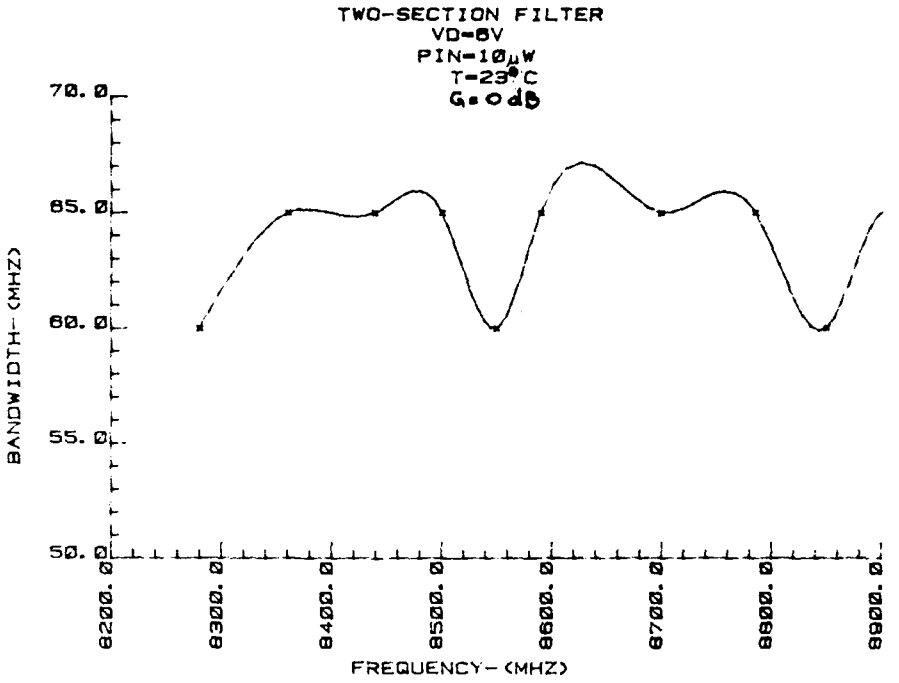

Figure 30. 3-dB bandwidth vs. frequency (two-section).

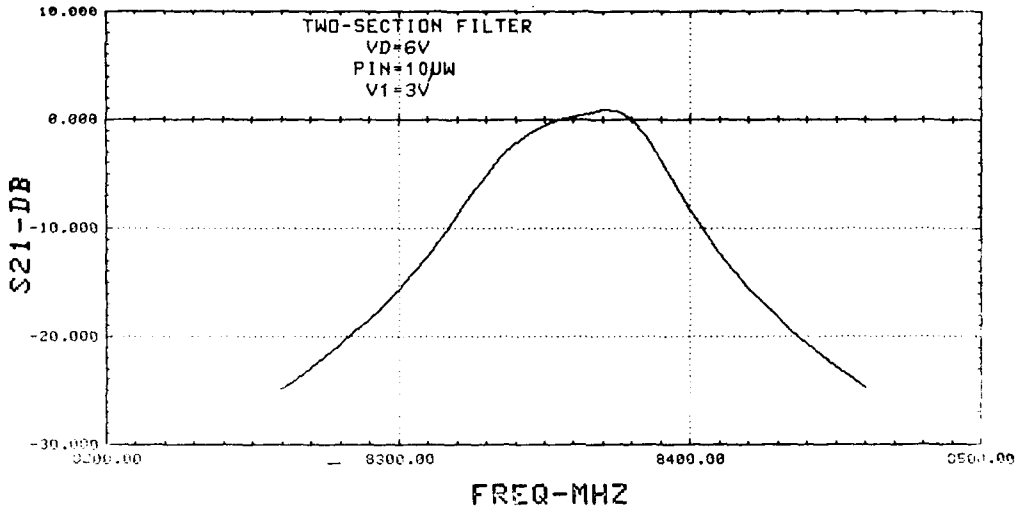

Figure 31. Transmission vs. frequency (V_v = 3 V).

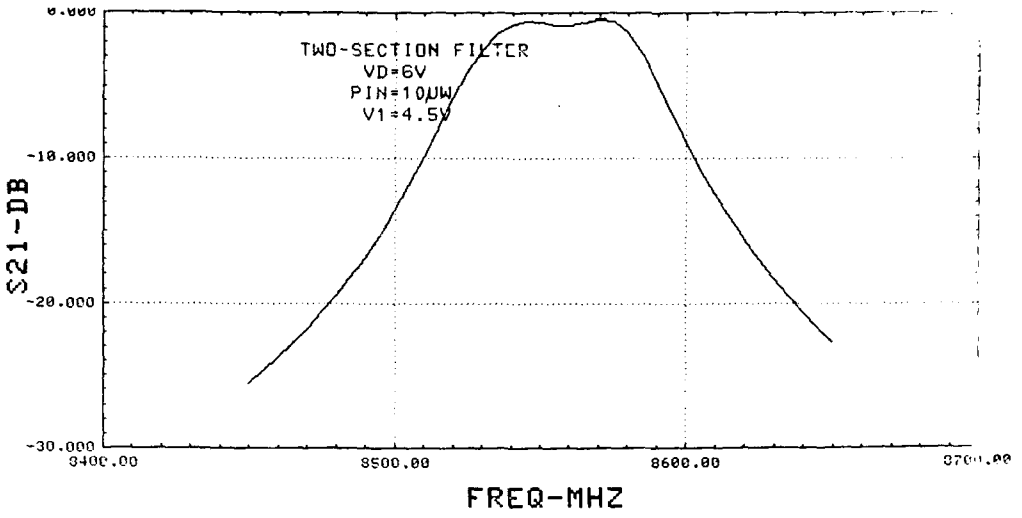

Figure 32. Transmission vs. frequency (V_v = 4.5 V).

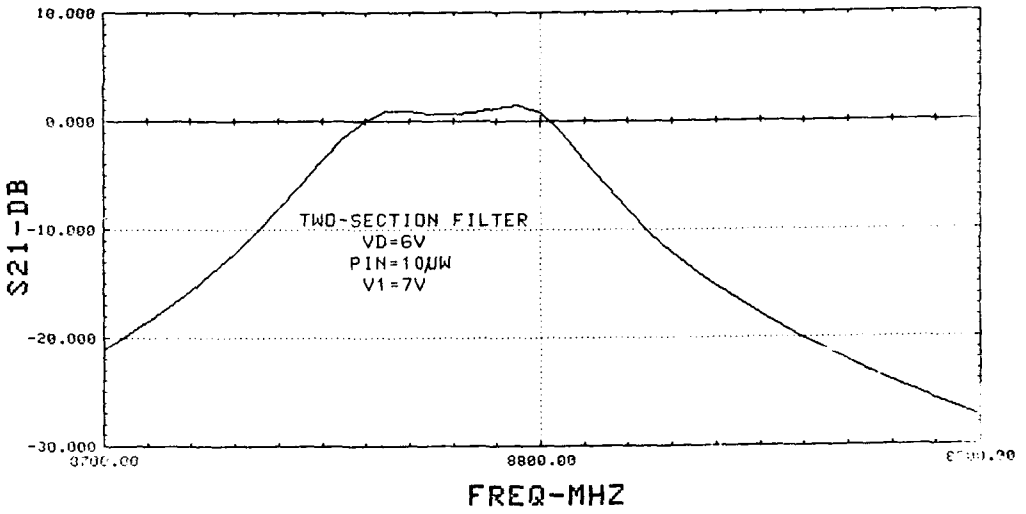

Figure 33. Transmission vs. frequency (V_v = 7 V).

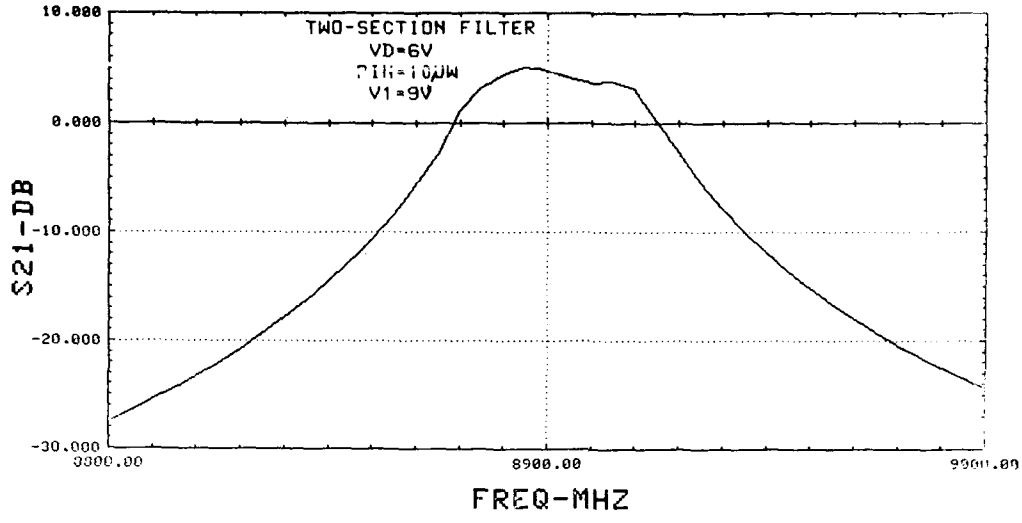

Figure 34. Transmission vs. frequency (V_v = 9 V).

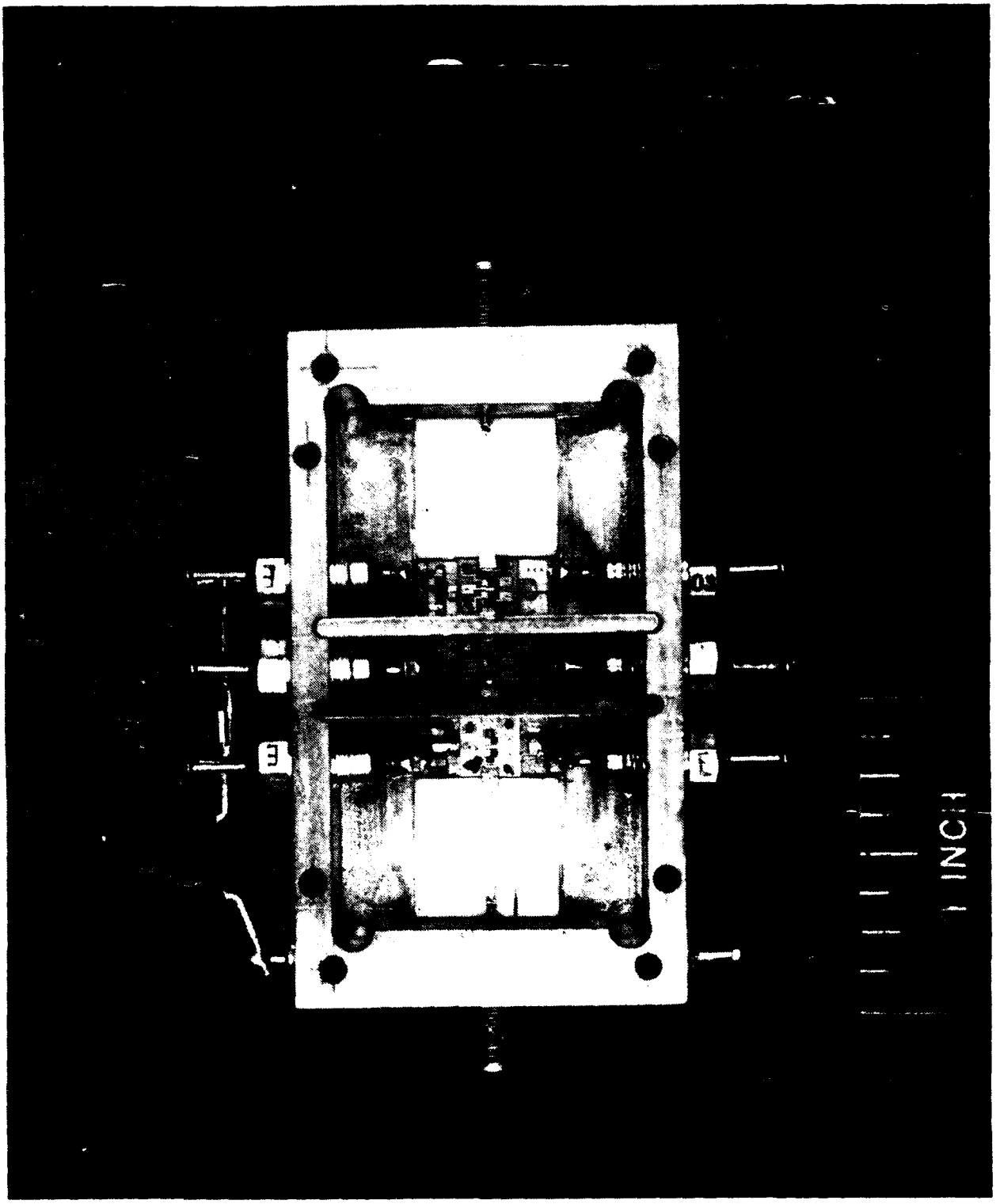

Figure 35. Three-section filter.

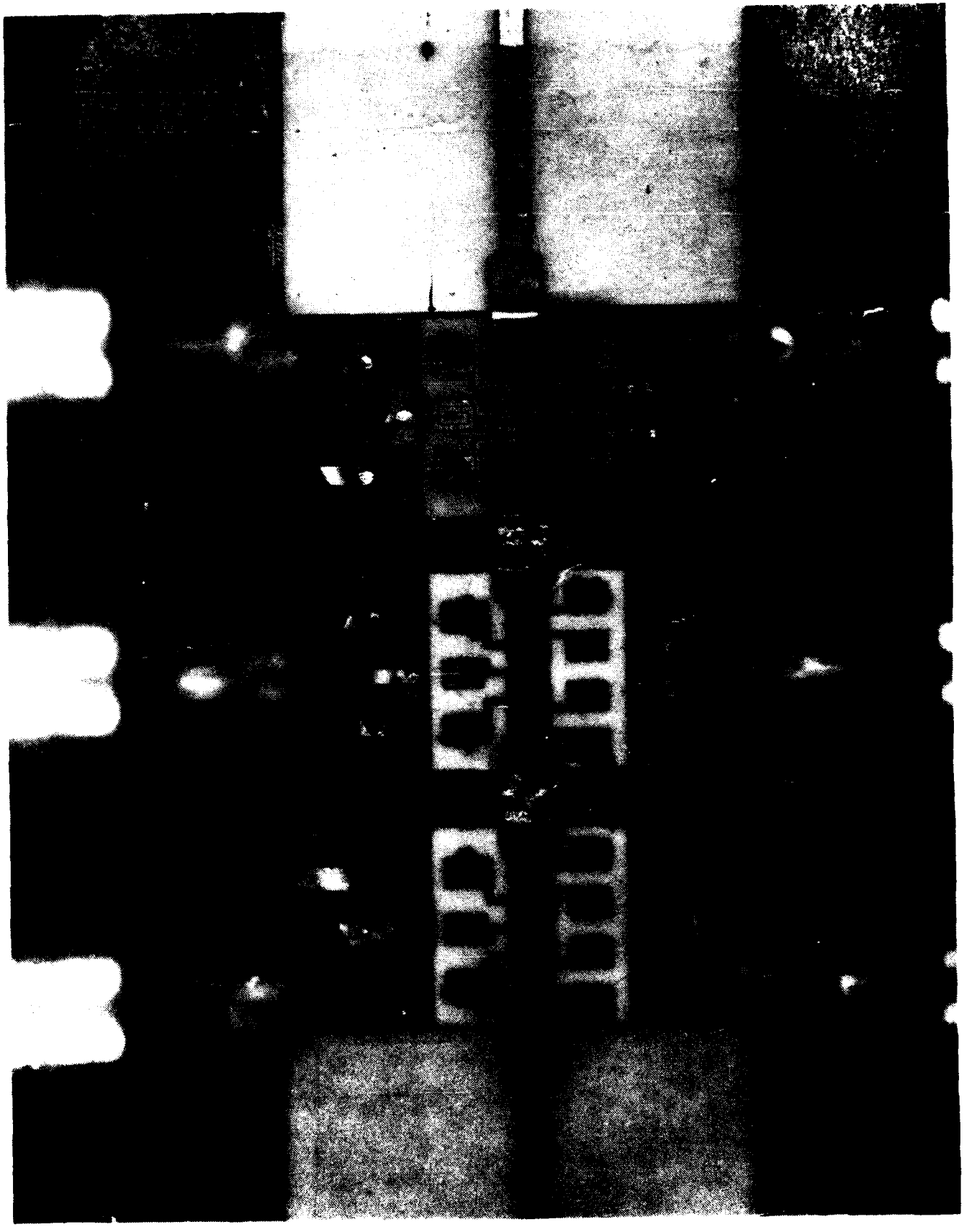

Figure 36. Close-up of three-section filter.

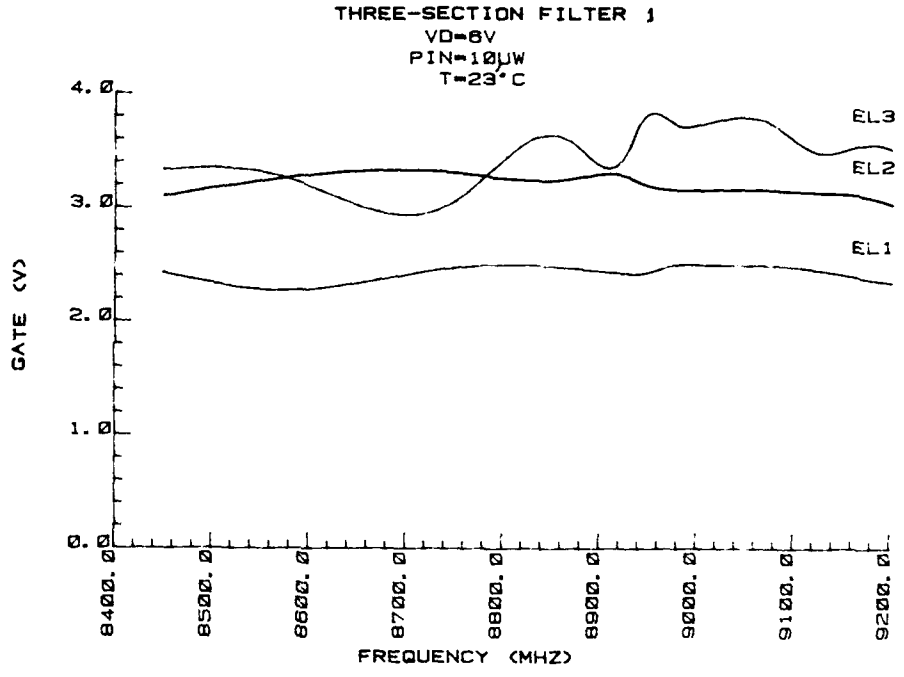

Figure 37. Gate voltage vs. frequency (unit 1).

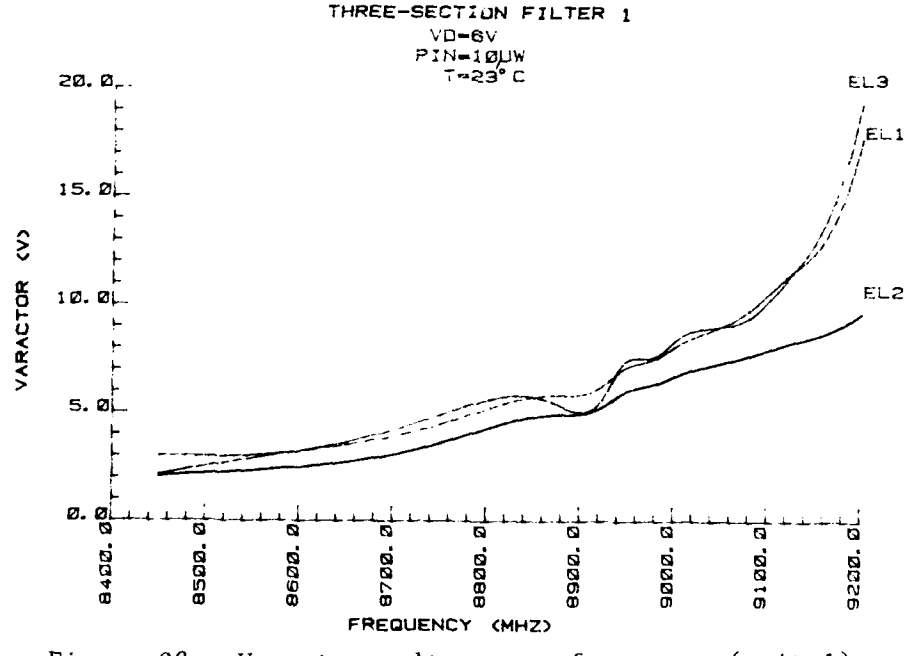

Figure 38. Varactor voltage vs. frequency (unit 1).

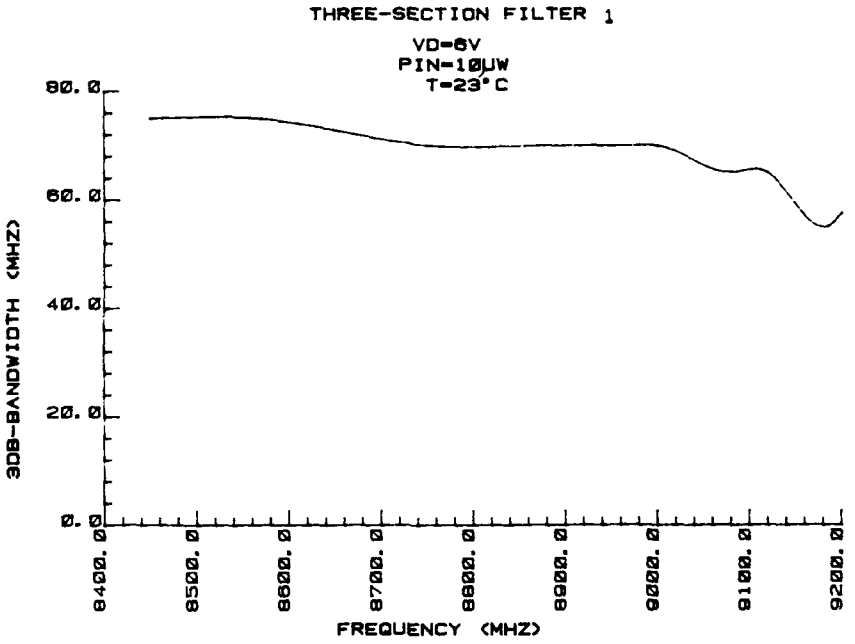

Figure 39. Bandwidth vs. frequency (unit 1).

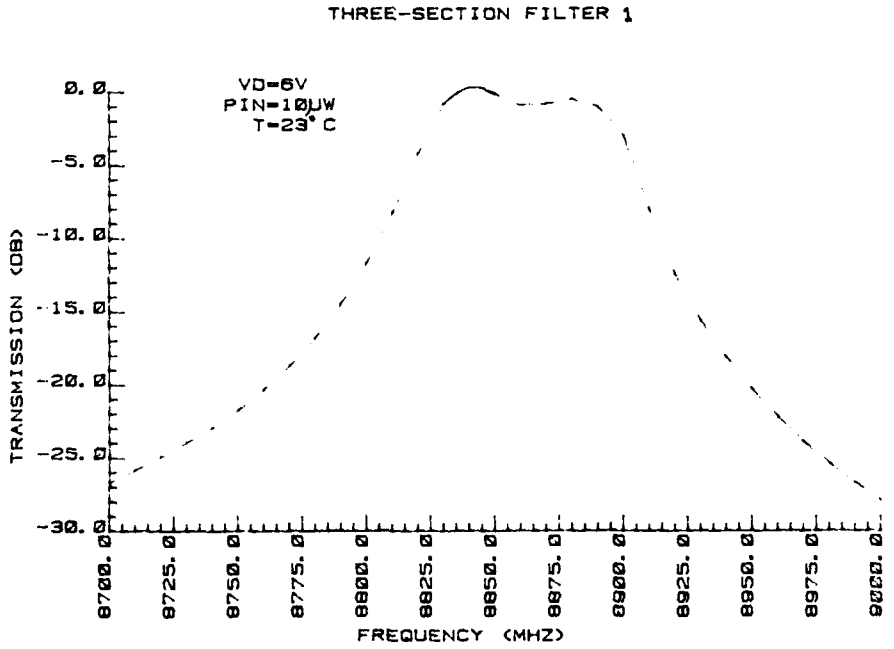

Figure 40. Transmission vs. frequency (F_o = 8850 MHz).

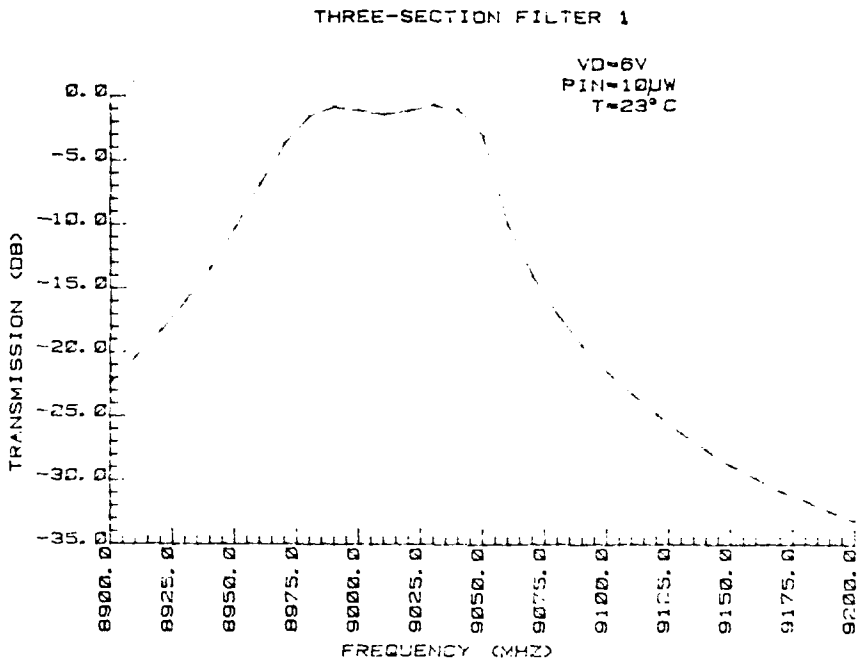

Figure 41. Transmission vs. frequency (F_o = 9000 MHz).

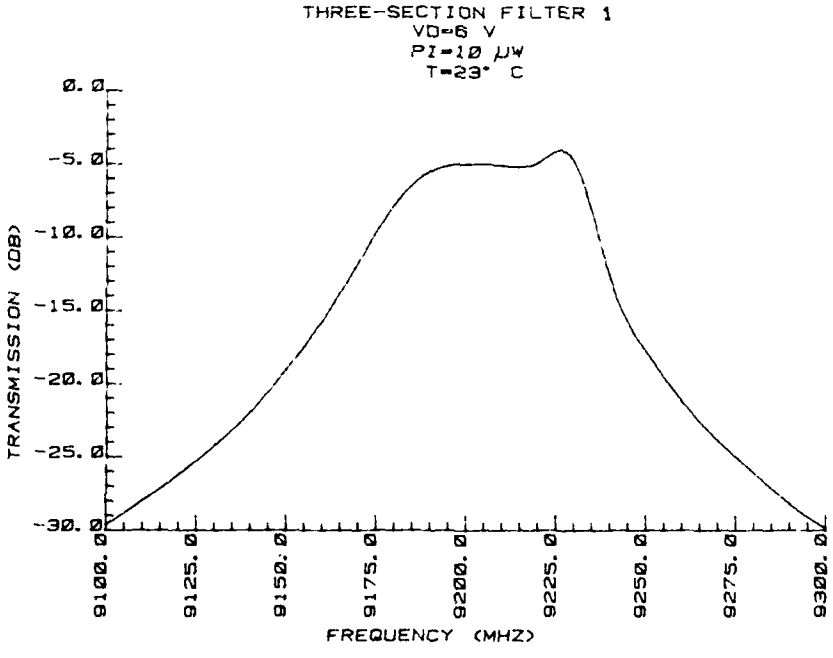

Figure 42. Transmission vs. frequency (F_o = 9200 MHz).

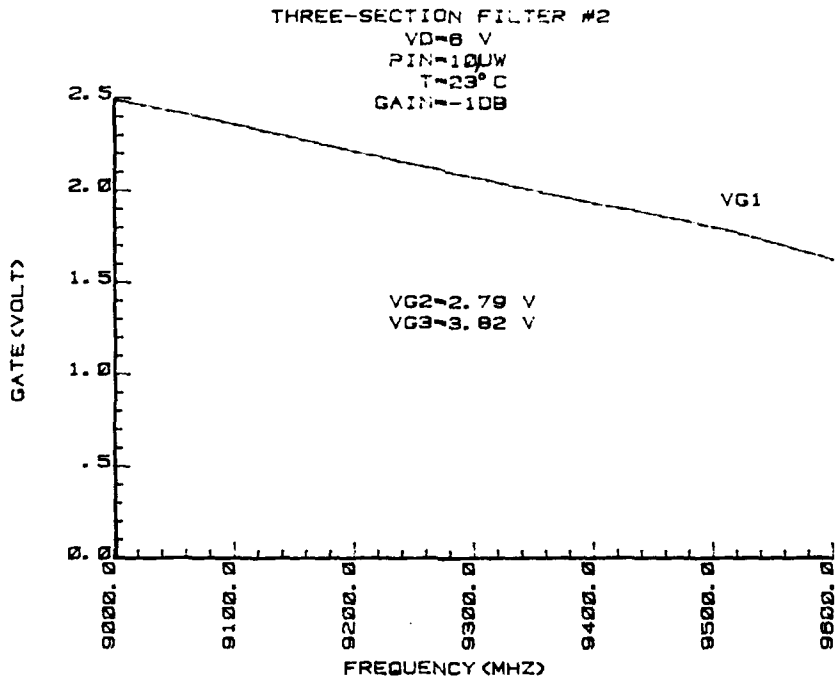

Figure 43. Gate voltage vs. frequency (unit 2).

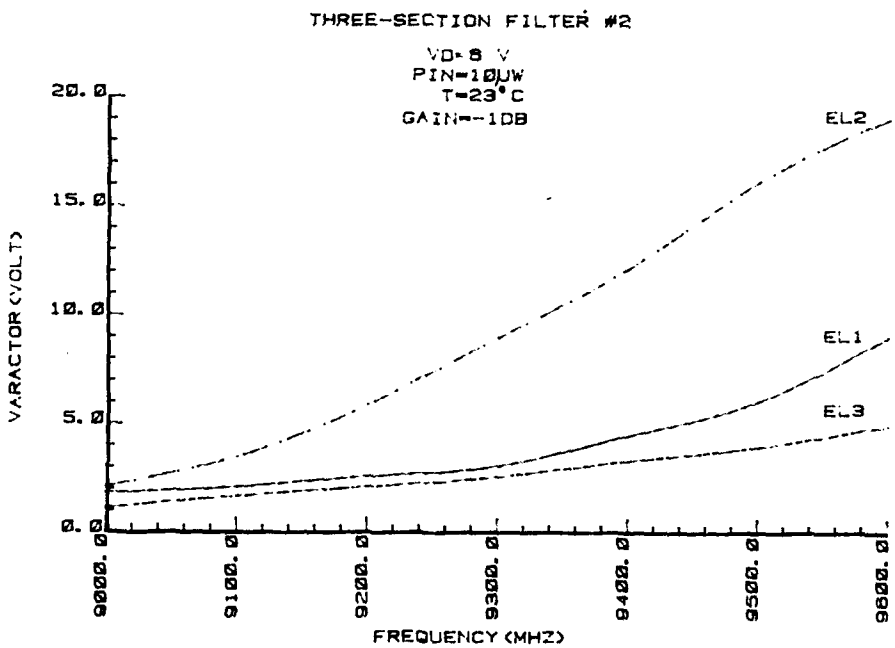

Figure 44. Varactor voltage vs. frequency (unit 2).

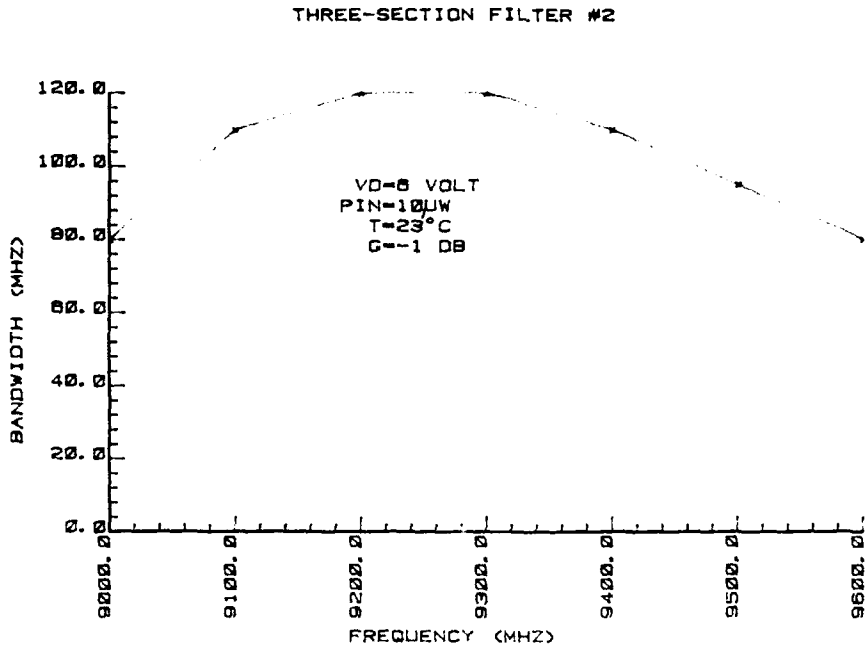

Figure 45. 3 dB bandwidth vs. frequency (unit 2).

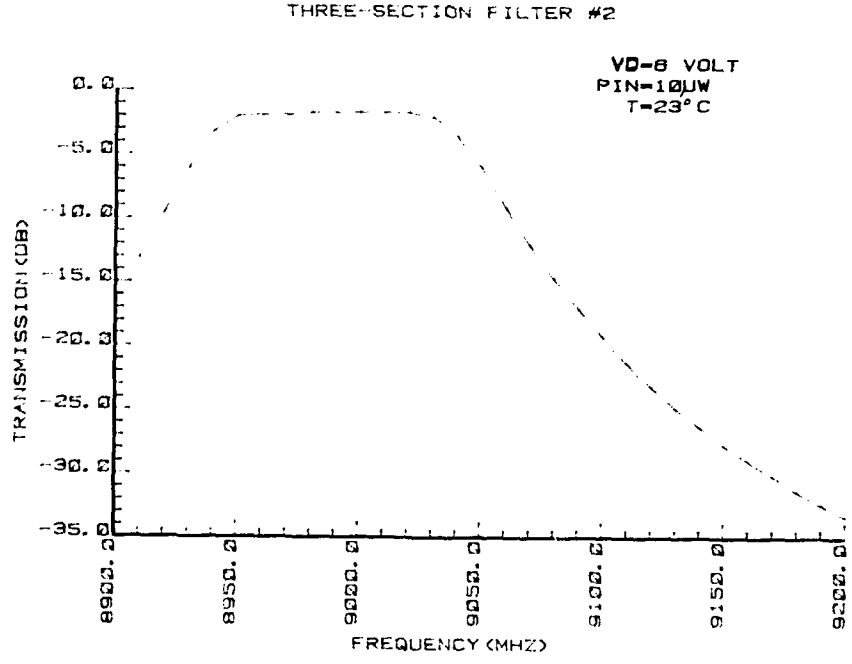

Figure 46. Transmission vs. frequency (F_o = 9.0 GHz).

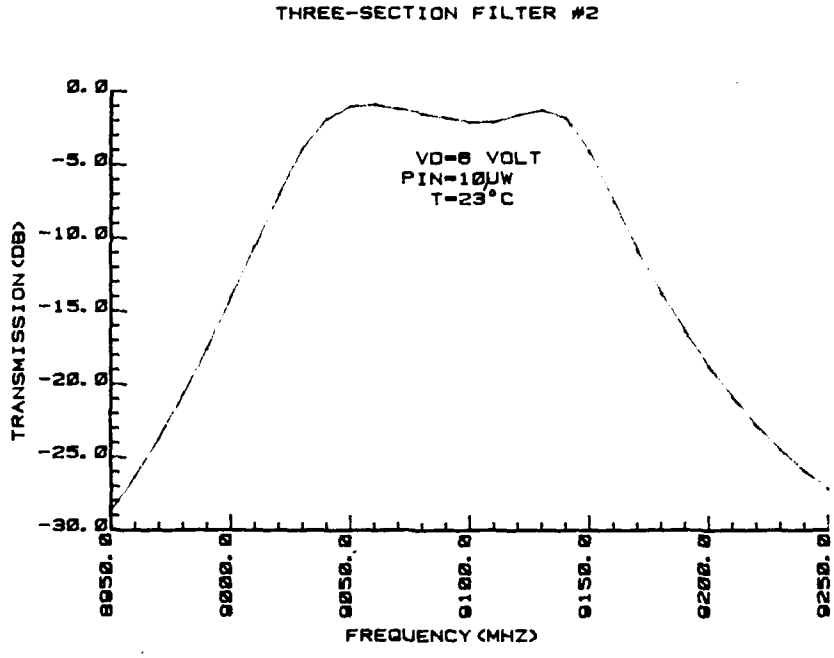

Figure 47. Transmission vs. frequency (F_o = 9.1 GHz).

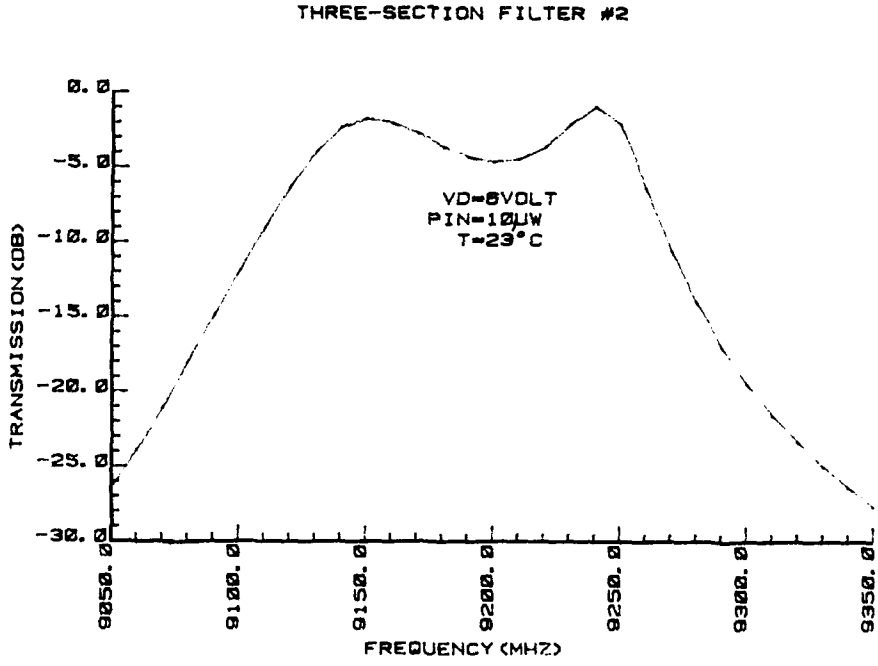

Figure 48. Transmission vs. frequency (F_o = 9.2 GHz).

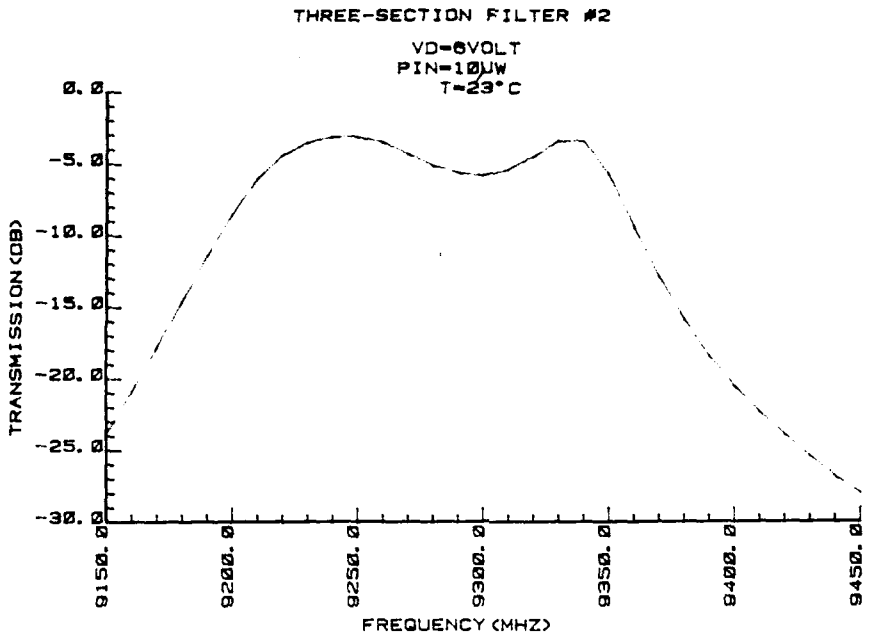

Figure 49. Transmission vs. frequency (F_o = 9.3 GHz).

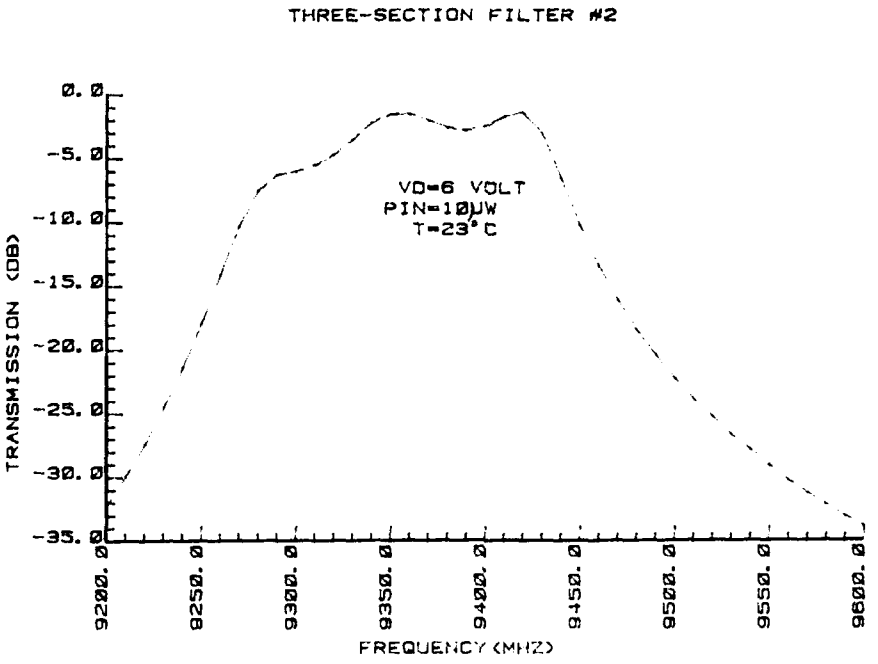

Figure 50. Transmission vs. frequency (F_o = 9.4 GHz).

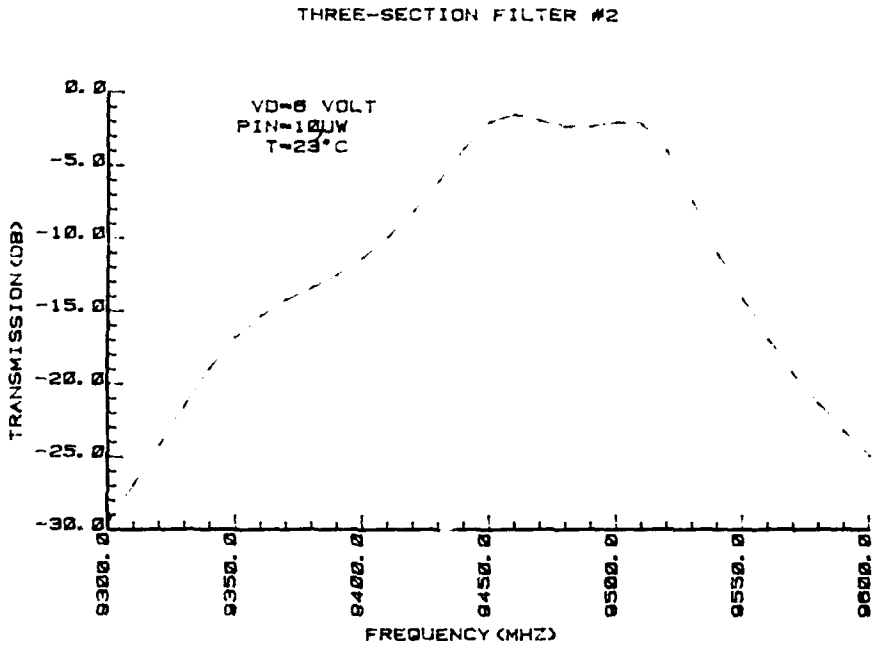

Figure 51. Transmssion vs. frequency (F_o = 9.5 GHz).

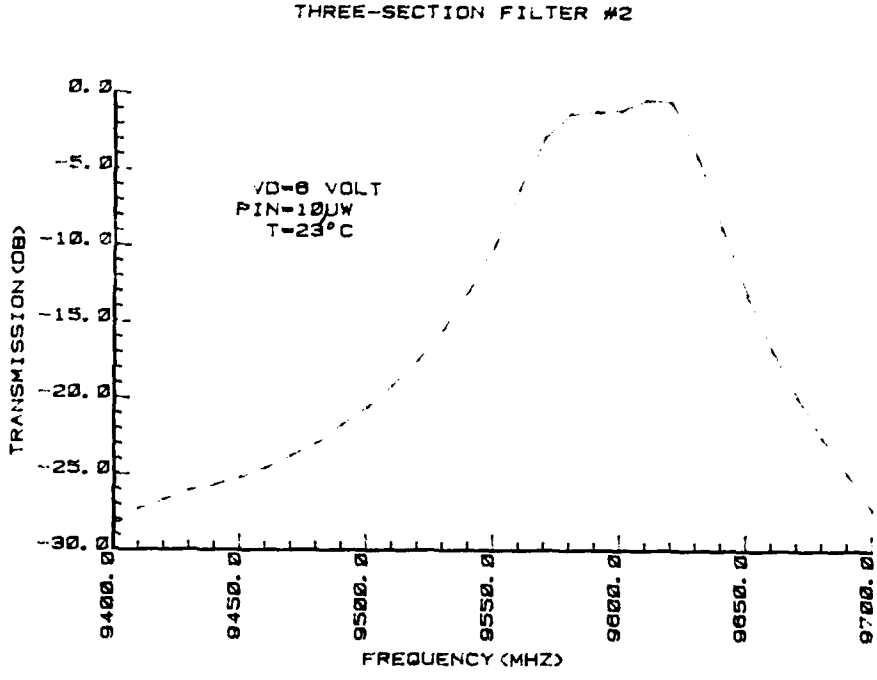

Figure 52. Transmission vs. frequency (F_o = 9.6 GHz).

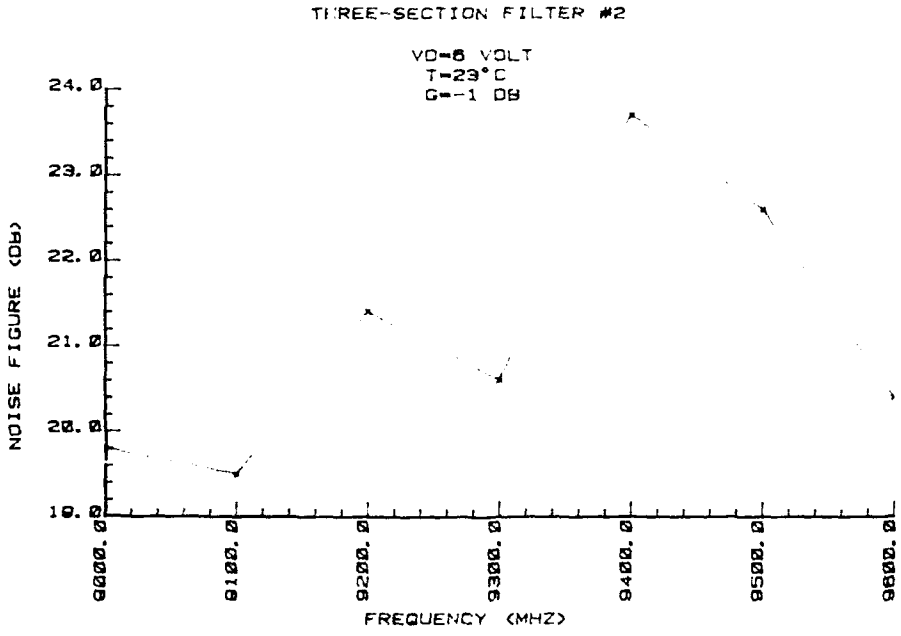

Figure 53. Noise figure vs. frequency.

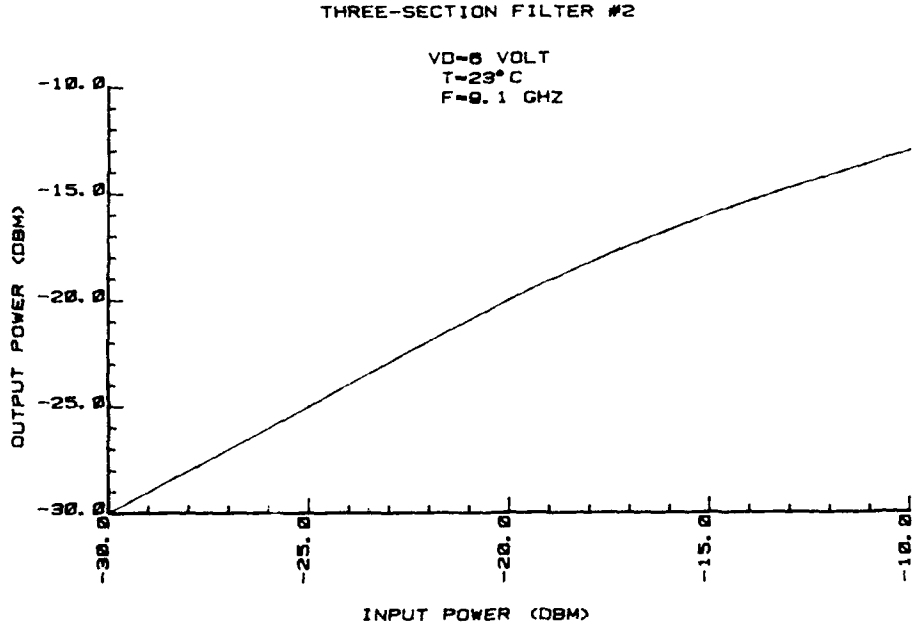

Figure 54. Output power vs. input power.

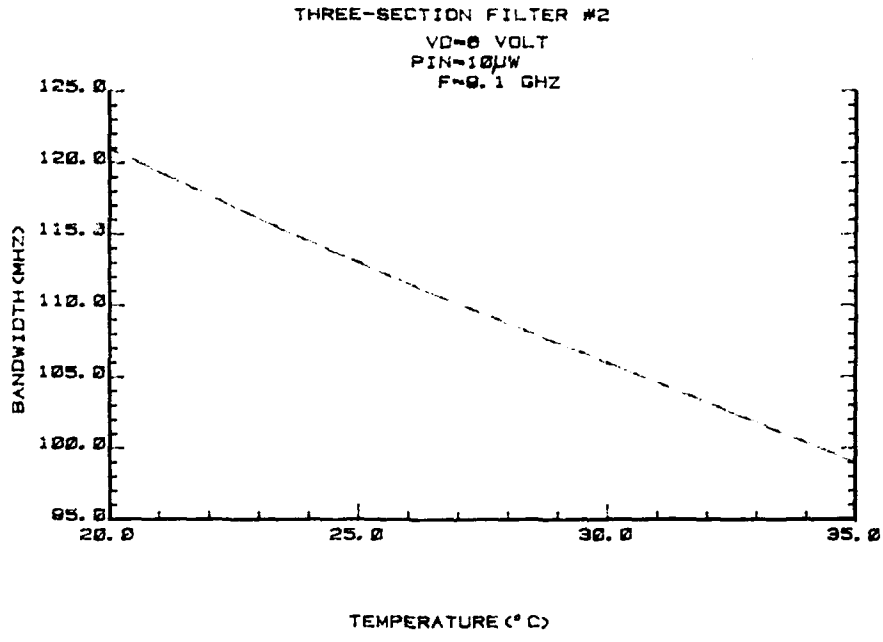

Figure 55. 3 dB bandwidth vs. temperature.

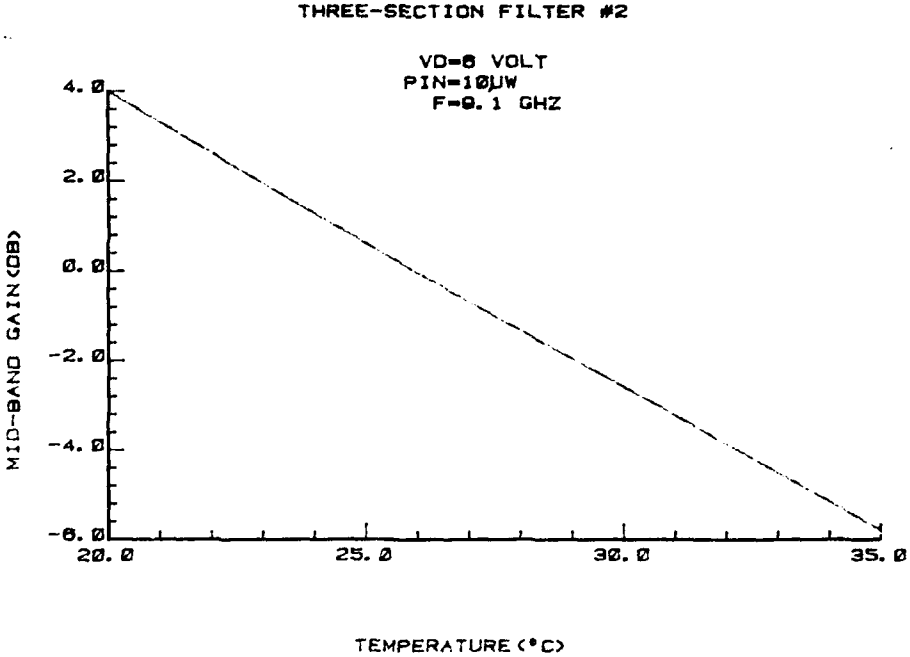

Figure 56. Midband loss vs. temperature.

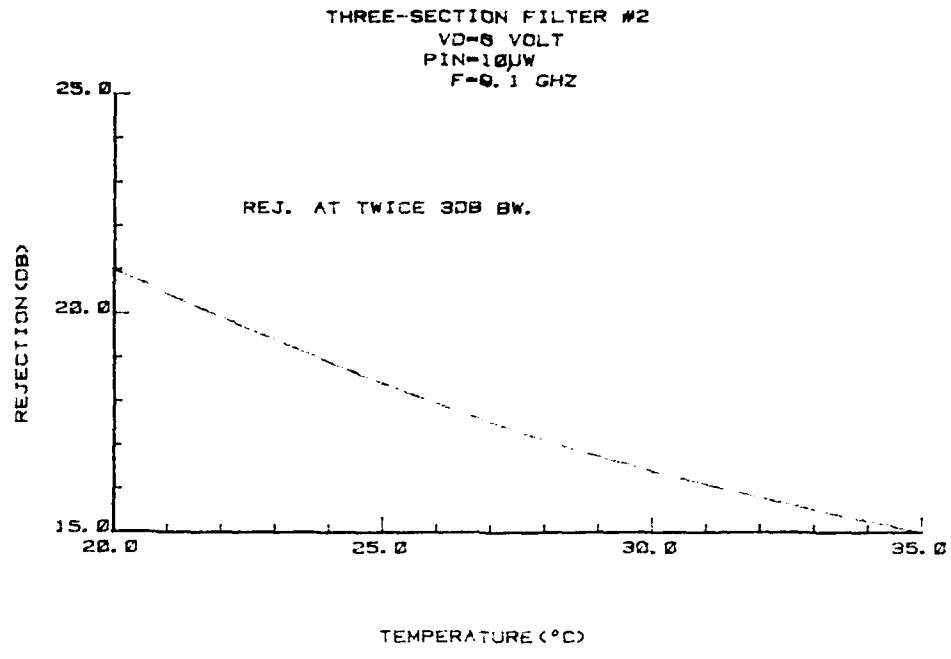

Figure 57. Rejection loss vs. temperature.

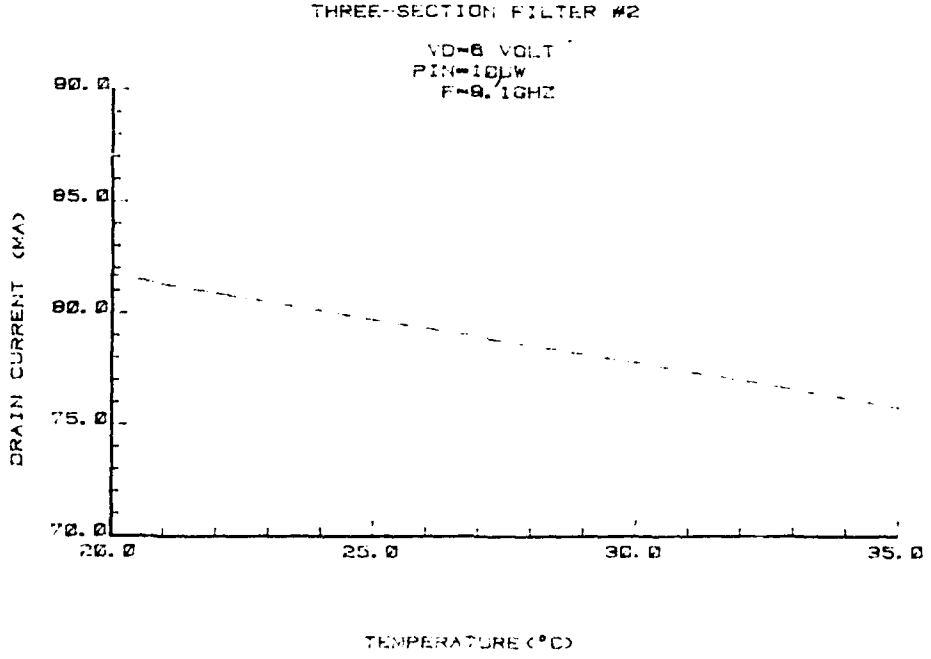

Figure 58. Drain current vs. temperature.

WPC No. 812762